Pergamon

Prog. Oceanog. Vol. 33, pp. 249-302, 1994

0079 - 6611/94 $26.00

(0079-6611(94) (0000)5-0

Boundary current instabilities, upwelling, shelf mixing and eutrophication processes in the Black Sea

HALİL İ. SUR, EMİN ÖZSOY AND ÜMİT ÜNLÜATA

Institute of Marine Sciences, Middle East Technical University, PK28 Erdemli, İçel, Turkey

Abstract – Satellite and *in situ* data are utilized to investigate the mesoscale dynamics of the Black Sea boundary current system with special emphasis on aspects of transport and productivity. The satellite data are especially helpful in capturing rapid sub-mesoscale motions insufficiently resolved by the *in situ* measurements.

Various forms of isolated features, including dipole eddies and river plumes, are identified in the satellite images. Unstable flow structures at these sites appear to transport materials and momentum across the continental shelf. Species differentiation and competition are evident along the boundary current system and at the frontal regions during the development of early summer productivity.

A time series of Coastal Zone Colour Scanner (CZCS) images indicate dynamical modulation of the springtime surface productivity in the southern Black Sea. Unstable meandering motions generated at Sakarya Canyon propag ite east with speeds of ~10-15km d^{-1}. Within weeks, a turbulent jet is created which separates from the coast, covering the entire southwestern sector. The nutrients driving the phytoplankton production (mainly *Emiliana huxleyi*) of the current system evidently originate from fluvial discharge entering from the northwestern region including the Danube river. The productivity pattern develops in early summer when the Danube inflow is at its peak, and through meandering motions spreads into an area several times wider than the continental shelf.

In 1980, the CZCS data, and in 1991 and 1992, the Advanced Very High Resolution Radiometer (AVHRR) data indicate patches of upwelling along the west Anatolian coastline between Sakarya Canyon and Cape İnce (*İnce Burun*) in summer. The upwelling phenomenon is outstanding because it occurs on a coast where normally the surface convergence near the coast implies downwelling, and under conditions of unfavourable winds.

In 1992, the hydrographic data indicated the upwelling to be the result of a surface divergence of the boundary current, and sequences of satellite data indicate the role of transient dynamics. The *in situ* data showed the upwelling centres to be devoid of phytoplankton as well as fish eggs and larvae.

The AVHRR and *in situ* hydrographic data in winter 1990 indicate cold water is formed over the entire western Black Sea continental shelf. The band of cold water decreases in width as it moves south and impinges on the headland at Baba Burnu, where it undergoes a sudden expansion. The maximum winter phytoplankton bloom sampled during the same period indicates explosive populations of diatoms following the band of cold water.

CONTENTS

1. INTRODUCTION

Exquisite observational detail of surface features is furnished by satellite remote sensing, an essential tool for studying dynamical processes often left unresolved by *in situ* measurements. This is especially true in the energetic environment of the Black Sea: whereas the *in situ* measurements yield 'hard' information, they necessarily lack sufficient resolution both in space and time to describe the rapidly changing mesoscale and sub-mesoscale fields. On the other hand, although satellite data may yield high resolution and time dependent information, this information is often qualitative and the results only describe surface features. It seems that the ultimate aim of reaching a sufficient understanding of the productivity and transport mechanisms operating in the Black Sea could only be accomplished by a synthesis of satellite and *in situ* data.

The high spatial frequency of sampling of the ocean surface with imaging sensors on board satellites has motivated detailed observations of complex oceanic processes. Although the ocean skin temperature measured by infra-red sensors (e.g. the Advanced Very High Resolution Radiometer - AVHRR) is frequently used to identify surface flow features in the ocean, diurnal solar heating can temporarily mask the ocean surface temperature, destroying any correlations with underlying dynamical features (e.g. DESCHAMPS and FROUIN, 1984). In addition, the heat stored by the surface mixed layer can be uniform in relatively large areas of the ocean, and therfore, many flow features may have a colour signature even when they do not appear on infra-red imagery (e.g. AHLNÄS, ROYER and GEORGE (1987).

In contrast, the CZCS collects data reflected from a depth range comparable with the attenuation distance of visible light in the ocean, and may thus give a better indication of the surface circulation (Appendix A). The CZCS was also a modern tool for assessing productivity in large areas of the ocean, though it must be recognized that phytoplankton pigments are not conservative tracers and often contain 'nutrient enrichment' effects in areas of the ocean where vertical mixing, density discontinuities, or upwelling of nutrients to within the photic zone lead to plankton growth (YENTSCH, 1984). In this way, they separate regions of increased fertility, which are typically the boundaries of major ocean currents or eddies. The transport patterns of plankton and suspended matter can serve to detect visually important features of the ocean current system, and are especially useful for studying interactions between the shelf and the deep ocean regions, because they allow

tracing of the pigment or suspended matter concentrations originating from coastal sources. Many collective programs recognize this potential of the analyses of the ocean colour as a tool of modern multi-purpose oceanographic assessments, e.g. the OCEAN Project aiming to develop a European colour data base and network (BARALE and FUSCO, 1992). The SeaWiFS ocean colour sensor expected to be operational in the coming decade is extremely promising for developing this technology further. In the Black Sea, comparative studies based on satellite and *in situ* data can reveal in full detail the ecological collapse stemming from eutrophication.

We use satellite and *in situ* data to identify a number of important dynamical processes in the Black Sea, and emphasize their impact on the biology and chemistry of the basin. As part of our discussion on the cross-shelf exchanges, we show filaments of river waters expanding from the shelf towards the deep basin region, among which are the ordered structures of dipole vortices. Similar oceanic dipole eddies have been illustrated by satellite observations elsewhere; for a review, the reader is referred to FEDOROV and GINSBURG (1989).

We also use satellite data in observing the features of the meandering boundary currents following the Black Sea basin periphery. Satellites have specifically been proved useful in similar environments where the rapid development and turbulent features can not be sufficiently resolved by *in situ* data. Unstable waves, meanders, dipoles, or paired eddies with opposite signed vorticity have frequently been reported along density-driven boundary currents in many parts of the world ocean: near Vancouver Island (THOMSON, 1984; IKEDA, MYSAK and EMERY, 1984), in the California Current (IKEDA and EMERY, 1985), off the southern coast of Alaska (AHLNÄS *et al*, 1987), in the Norwegian Coastal Current (CARSTENS, MCCLIMANS and NILSEN 1984; JOHANNESSEN, SVENDSEN, JOHANNESSEN and LYGRE, 1989; IKEDA, JOHANNESSEN, LYGRE and SANDVEN, 1989), in the Sea of Okhotsk and the Subarctic Polar Frontal Zone (FEDOROV and GINSBURG, 1989), in the Fram Strait Marginal Ice Zone (JOHANNESSEN, JOHANNESSEN, SVENDSEN, SCHUCHMAN, CAMPBELL and JOSBERGER, 1987; GINSBURG and FEDOROV, 1989), off the Labrador Coast (IKEDA, 1987), in the East China Sea (QIU, IMASATO and AWAJI, 1988), in the Leeuwin Current along western Australia (CRESSWELL and GOLDING, 1980; LEGECKIS and CRESSWELL, 1981; THOMPSON, 1984; GRIFFITHS and PEARCE, 1985), along the Ligurian Coastal Current (CREPON, WALD and MONGET, 1982), and along the Algerian Current (MILLOT, 1985, 1991).

An interesting consequence of the boundary current instability, of interest in the Black Sea, is the rather unexpected patterns of upwelling generated in summer. Similar transient features of unexpected upwelling has been found along boundary current systems by QIU *et al* (1988) and CHAO (1990), and near anticyclonic members of coastal eddy pairs along the Algerian Current (MILLOT, 1991; BECKERS and NIHOUL, 1992).

In addition to the basic baroclinically unstable flow situations reviewed above, the interaction of a boundary current with the coastline geometry, or with the continental shelf/slope topography appears to be another possible mechanism that could lead to the unstable meanders, eddies or filaments along the Black Sea periphery. A review of similar situations is given in the sequel, together with the interpretation of our observations.

Whatever may be the cause leading to the meandering and filamented structures of boundary currents, they are of primary importance in determining the exchange between the shelf regions and the deep ocean, with many biogeochemical implications. In a basin of relatively small size such as the Black Sea, cross-shelf exchanges are of central importance because (1) occasionally the horizontal scales in the bursts of exchanges are almost of the same scale as the basin itself, (2) a significant amount of the fresh water nutrients and other materials are inputed from major rivers (e.g. the Danube), and advected along the coast by the boundary current, finally being injected into the basin interior via turbulent exchanges.

The methods of observation and image analysis are discussed in Section 2. A description of the general features of the Black Sea circulation, river inputs, and productivity are given in Section 3. The results of our analyses are described in Section 4. In Section 4.1 we illustrate the effects of river plumes and describe cross-shelf transport caused by mushroom eddies. Then, in Section 4.2 we discuss the rapid development, separation and disintegration of a meandering jet flow along the Anatolian coast. Local upwelling along the same coast is discussed in Section 4.3. Winter mixing on the continental shelf, and the interactions with coastline geometry are described in Section 4.4. From the observations, we extract information concerning the impacts on productivity and eutrophication processes. Conclusions and discussion can be found in Section 5.

2. THE SATELLITE IMAGERY AND METHODS

Nimbus-7 CZCS and NOAA AVHRR images are used to infer the flow characteristics of the Black Sea boundary current. Imagery produced by visible and thermal sensors of these satellites are used to investigate regional flow dynamics by comparative studies of the optical and thermal properties. The processing details and the basis for the interpretations of these satellite data are given in Appendix A.

All of the image processing was done on the SEAPAK interactive processing system at the Institute of Marine Sciences, Middle East Technical University, excluding the images presented in Figs 19d,e which were processed by the KNMI (Royal Netherland Meteorological Institute). Approximately 100 relatively cloud free images of the Nimbus-7 CZCS and NOAA AVHRR were examined and geometrically transformed to Mercator projection.

The NOAA-10 thermal infra-red images could not be corrected for atmospheric effects because of the inapplicability of the method for this particular satellite; in these cases the images have been used with contrast enhancement of relative sea surface temperatures, resulting in east-west temperature gradients depending on solar and satellite altitude. Only a few NOAA-11 images were available (Figs 19d,e). The Nimbus-7 CZCS served as a secondary source of infra-red data, interpreted only in terms of relative temperatures since the radiometric performance of this sensor has been questionable (ROBINSON, 1991). A third source of data was the NOAA APT transmissions.

3. A BRIEF REVIEW OF THE CIRCULATION AND PRIMARY PRODUCTIVITY

3.1 Bottom topography

The bottom topography of the Black Sea basin is shown in Fig.1. The abyssal plain (depth >2000m) is separated from the margins by steep continental slopes, excluding the gentler slopes near the Danube and Kerch Fans. The wide northwestern continental shelf (mean depth ~50m) occupies the region between the Crimean peninsula and the west coast. This wide continental shelf extends along the western and southwestern coasts of the Black Sea with depth <100m at the shelf break. In fact the entire western Black Sea shelf extending from Crimea to the Sakarya River on the Anatolian coast is a continuous region of flat topography decreasing in width towards its southern terminus. The shelf becomes abruptly terminated at Sakarya Canyon, an abrupt feature where the depth suddenly increases from 100m to about 1500m along the Anatolian coast east of the Bosphorus. The canyon is delimited by Baba Burnu (Cape Baba) on its east, where the coast makes a sharp turn. Smaller continental shelf areas are found along the coast between the two Capes of Kerempe Burnu and Bafra Burnu, along the coast of Kerch, and at narrow stretches separated by canyons along the eastern coasts.

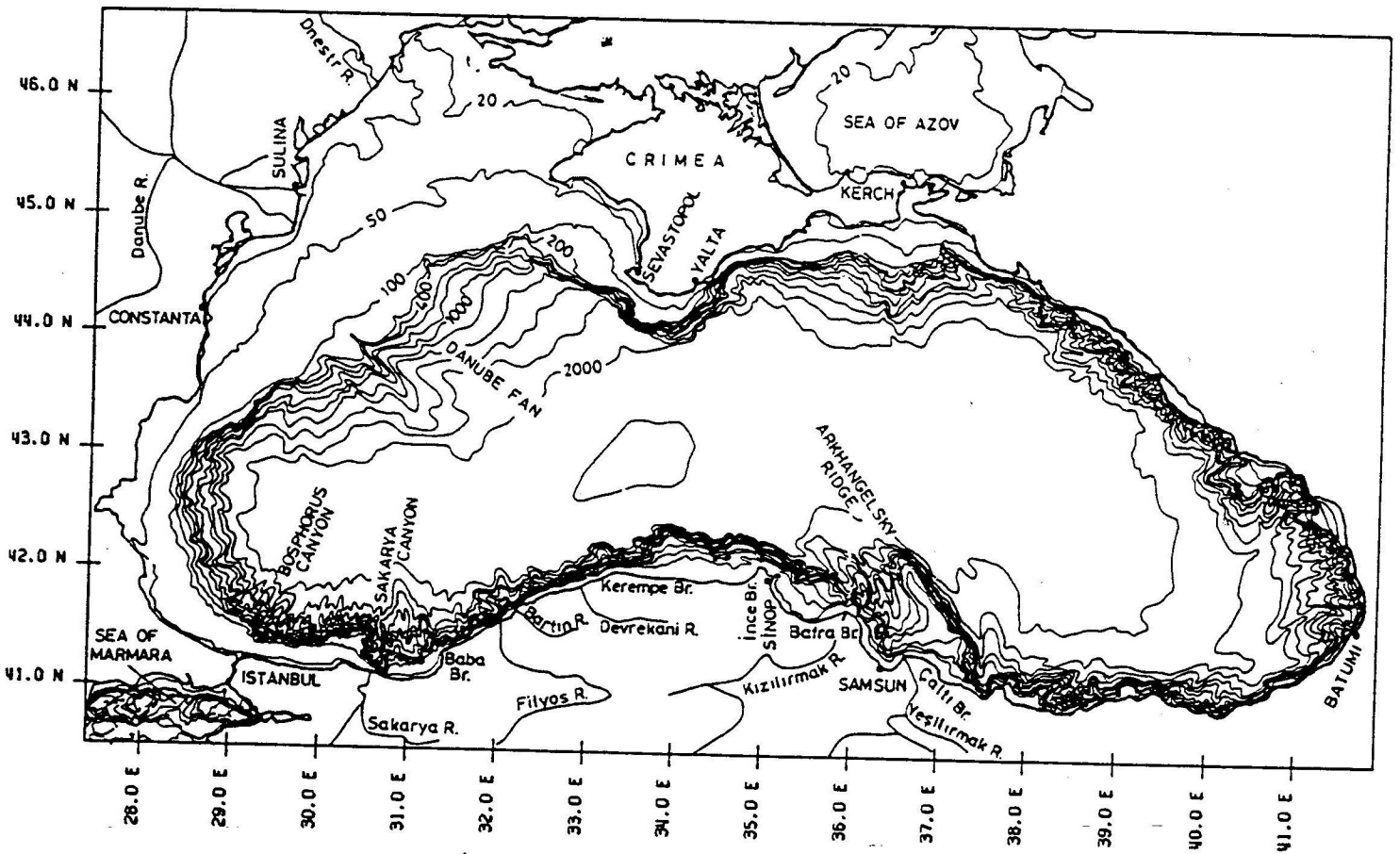

FIG. 1. Bathymetry and location map of the Black Sea.

Along the coast from Sakarya Canyon to Cape Kerempe, a steep continental slope topography is located adjacent to the coast. The cross-shore depth profile changes from a flat, step shaped continental shelf topography west of the Sakarya Canyon to a steep linearly deepening profile following the coastline between Sakarya Canyon and Cape Kerempe, and back to the step-like shelf profile west of Cape Kerempe. These transitions in bottom topography induce significant control on the dynamics of the boundary currents, as will be shown in Section 4.2.

The bottom topography becomes complicated near the Arhangelsky Ridge, a prominent deep feature (shallowest contour at 400m) east of the central Anatolian (Sinop) shelf; then along the remaining eastern Black Sea coast, the continental slope topography undulates between shallow and deep regions. The continental slope region is intersected by numerous canyons throughout the Black Sea.

3.2 The general circulation

A basin scale cyclonic boundary current is the main feature of the Black Sea general circulation. KNIPOVICH (1933) and NEUMANN (1942) were the first to note a division of the circulation pattern into two large cyclonic gyres in the eastern and western halves of the basin, with smaller scale circulations between the two gyres and in the easternmost corner of the basin. BLATOV, KOSEREV and TUZHILKIN (1980) confirmed this circulation and indicated that the centre of the eastern gyre was displaced to the west in summer. According to LATUN (1990), the winter circulation is stronger and better organised than in the summer, when increased mesoscale eddy activity breaks or masks the continuity of the basin circulation. STANEV's (1990) results also support this intensified winter circulation.

It is not clear what physical factors drive the Black Sea circulation. Classically, cyclonic winds (positive curl of wind stress) have been recognized as the main reason for the cyclonic surface circulation (e.g. NEUMANN, 1942; MOSKALENKO, 1976). On the other hand, the results of numerical studies by MARCHUK, KORDZADZE and SKIBA (1975) and STANEV (1990) indicate a seasonal thermohaline circulation driven by nonuniform surface fluxes, complementary to the wind driven circulation, and generating surface currents of comparable magnitude.

Relatively little is known on the role of freshwater runoff from major rivers in establishing a density driven component of the circulation. Although their effects are suspected to be of secondary importance, both the river inflows and the Bosphorus fluxes are expected to modify the circulation through local effects superimposed on the horizontal and vertical ambient stratification.

The northwestern shelf and the Bosphorus vicinity are the two major areas where lateral sources and convection modify the Black Sea circulation (STANEV, 1990). The competing effects of freshwater inflow and winter cooling respectively create and destroy vorticity in the first area, while intermediate depth intrusions driven by shelf mixing of the dense Mediterranean inflow (ÖZSOY, ÜNLÜATA and TOP, 1993) create disturbances including vertical motions in the second area. In both regions, the eddy kinetic energy increases at the expense of mean kinetic energy (STANEV, 1990).

While GAMSAKHURDIYA and SARKISYAN (1976) found the joint effect of baroclinicity and bottom relief (the 'jebar' effect) to be the most important factor in the dynamics of the Black Sea general circulation, the results of STANEV (1990) did not indicate a significant contribution, which according to the author was a result of the strong vertical stratification in the Black Sea. We suggest that these conflicting interpretations could result from insufficient resolution of either the topography or the density structure in the models, because observations often suggest that the core of the boundary current with the largest horizontal density gradients coincides with the narrow continental slope topography. Slope currents are quite common elsewhere, and a fair understanding of their dynamics exists; see HUTHNANCE (1992) for a review.

Mesoscale eddies are known to exist in the Black Sea, and are subject to large excursions and mutual interactions. Central basin features formed by merging of anticyclonic eddies shed from the coherent flows along the northern and southern coasts have been demonstrated by LATUN (1990) and GOLUBEV and TUZHILKIN (1990). Mesoscale eddies of stationary and travelling forms are also indicated by OGUZ, LA VIOLETTE and ÜNLÜATA (1992). In fact the eddies are an integral part of the boundary currents, and lead to the meandering of this current, as noticed earlier by BLATOV *et al* (1984).

The upper ocean circulation derived from recent hydrographic measurements (OGUZ, LATUN, LATİF, VLADİMIROV, SUR, MARKOV, ÖZSOY, KOTOVSHCHIKOV, EREMEEV and ÜNLÜATA 1993) is described by a well defined cyclonic boundary current approximately following the narrow continental slope region and a series of semi-permanent anticyclonic eddies on the periphery between the boundary current and the undulations of the coast (Fig.2). Of these the Batumi anticyclonic circulation is the most prominent closed circulation, existing in the eastern corner of the Black Sea for most of the time, and this is the only region where the cyclonic boundary current ceases to follow the basin slope boundary. This interpretation attempts to generalize the steady general circulation, assigning quasi-permanent anticyclonic cells to the periphery, which in our opinion is associated with the meandering structure of the boundary current, leading to standing structures as well as transient features.

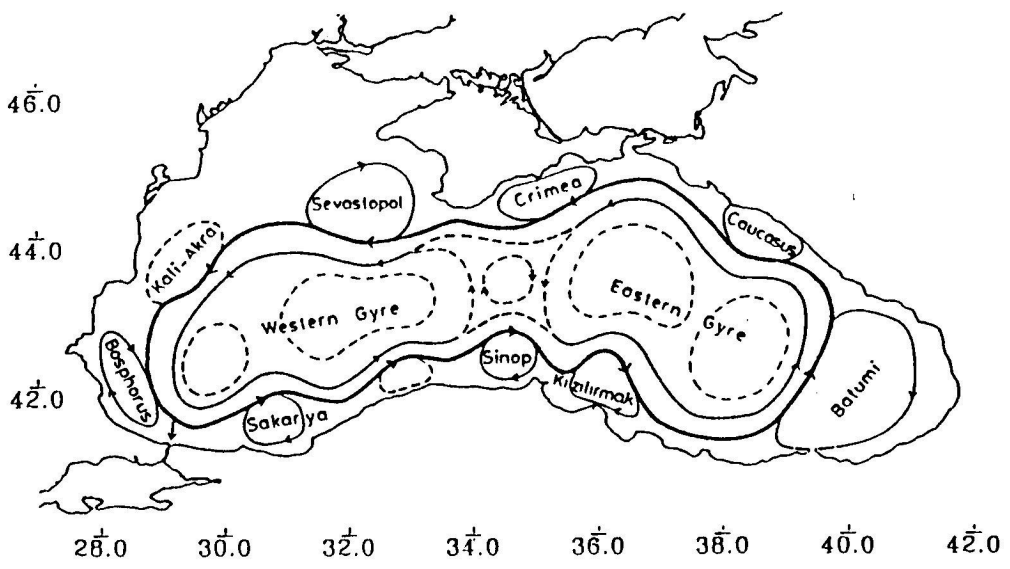

FIG.2. Schematized general circulation of the Black Sea (after OGUZ *et al*, 1993).

3.3 The effects of riverine discharges in the western Black Sea

Major rivers (the Danube, Dnepr and Dnestr) discharge into the northwest shelf of the Black Sea (the region between Crimea and Romania). The Danube River is the greatest contributor of river run off into the Black Sea, accounting for about one half of the total riverine influx. The total discharge of the Dnestr and Dnepr rivers is about a third that of the Danube, and the total discharge of the remaining rivers accounts for a small fraction (<1/5) of the total river runoff.

The annual mean discharge of the Danube, monitored for more than a century (Fig.3a) indicates large natural fluctuations within the range of 4000-9000m^3s^{-1}. In addition to this interannual variability, seasonal changes of about ±30% of the annual mean occur in the discharge (SERPOIANU, 1973; ÖZTURGUT, 1966; TOLMAZIN, 1985; BONDAR, 1989; SERPOIANU, NAE and MALCIU, 1992). Therefore one can expect variations of up to ~3-fold between the minimum and maximum seasonal discharges. The annual Danube influx is well correlated with the basin sea-level (Fig.3b) on seasonal and interannual time-scales (BONDAR, 1989). ÖZSOY (1990) and ÖZSOY, LATİF, TUGRUL and ÜNLÜATA (1992) suggest that the nonlinear mechanism of hydraulic controls imposed by the Bosphorus results in the long-term response of the mean sea level to net freshwater inflow. In addition, SERPOIANU *et al* (1992) show that the salinity decrease measured at Constanza (downstream of the Danube) is also closely correlated with the Danube discharge on seasonal and interannual time scales (Figs 3c,d). The Danube water usually flows cyclonically (to the south) around the basin, except during storms when strong southwesterlies push its waters back into the northwest shelf (TOLMAZIN, 1985).

Salinity data from near the Anatolian coast suggest that the freshwater from the northwest shelf reaches the southwest coast. Daily measurements in the Bosphorus (Figs 4a,c) indicate minimum salinity at different periods of each year, from spring to late summer (ACARA, 1958; ARTÜZ and OGUZ, 1976). Although salinity minima can be observed as early as March-April, the more prominent salinity minima are observed during summer, from June till September. The mean travel time between the Danube and the Bosphorus (~500km) is calculated to be on the order of 1-2 months assuming a mean current speed of 10-20cm s^{-1}. The irregularities and lags in the timing of minimum salinity waters observed along the Anatolian coast could result from mixing and dispersion effects of the circulation transporting the northwest shelf waters south.

To show the river effects, we computed the mean salinity of the surface waters within the upper 10m (Fig.5a) in the southwestern Black Sea (between 28° and 32°E, and 41° and 42°N) from the detailed coverage of the R/V *Bilim*, the research vessel of the Institute of Marine Sciences, Middle East Technical University, during 1985-1992, including offshore and inshore stations, as well as stations in the Bosphorus, where more frequent measurements were obtained. The weight of the data indicates a mean salinity of about 18 in the southwest sector of the Black Sea. The salinity decreases to 16-17 during the exceptional conditions when the Danubian influence is felt in the area. The minimum salinity periods in Fig.5a occur at different times varying from March to August each year, which are superposed in the seasonal plot of Fig.5b.

3.4 Primary production and eutrophication processes

A number of complex factors control the spatial/temporal distribution, variability and recycling of the primary production in the Black Sea, including the peculiar redox processes and their bacterial mediation at the oxic-anoxic interface, the vertical and horizontal transport of nutrients originating from the riverine, atmospheric and land sources, and their exchanges between the shelf and deep waters.

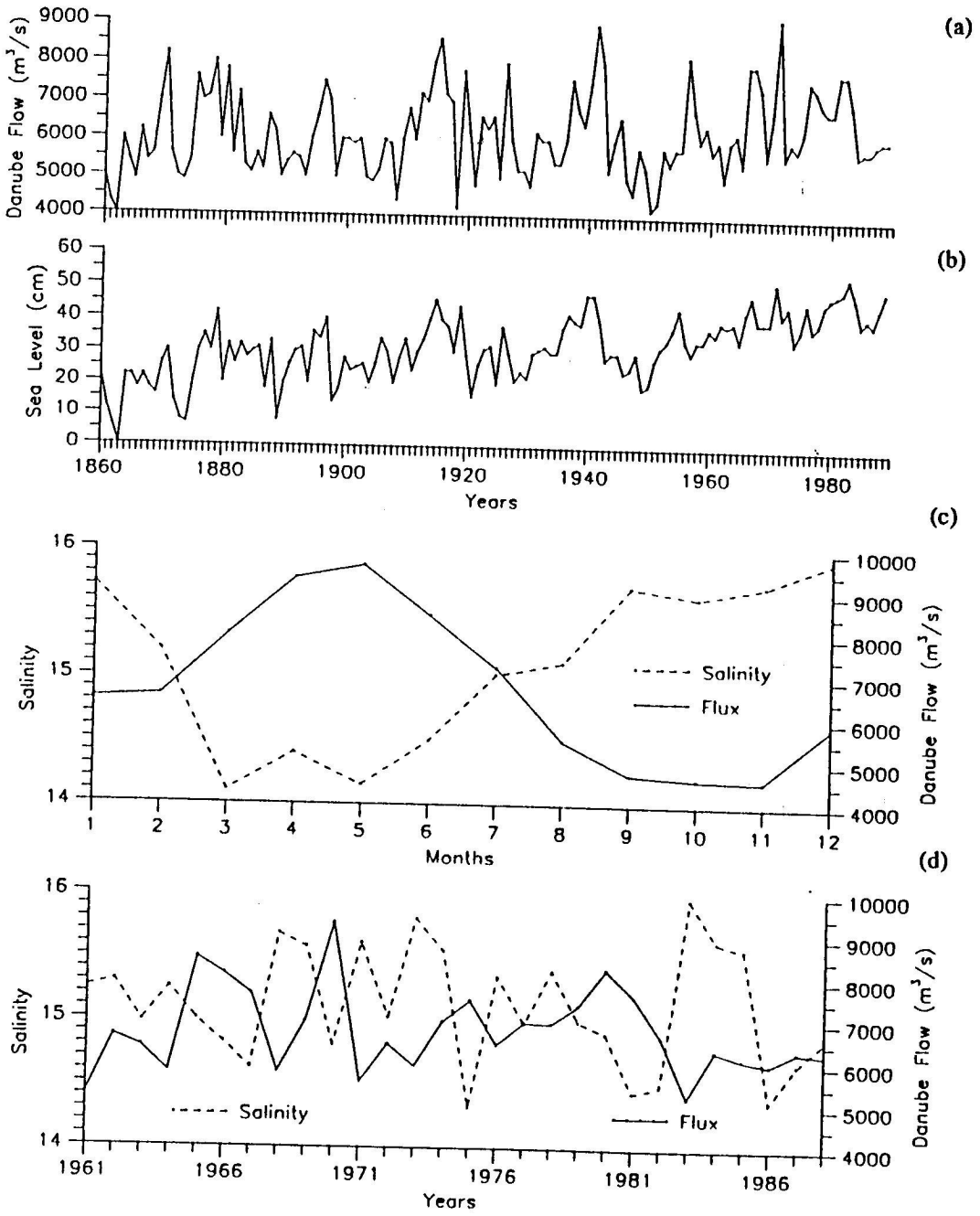

FIG.3. Long-term measurements of annual average (a) Danube discharge, (b) sea level at Sulina on the Romanian coast (after BONDAR, 1989), (c) monthly average and (d) annual average Danube discharge and salinity at Constantza, Romania (after SERPOIANU *et al*, 1992).

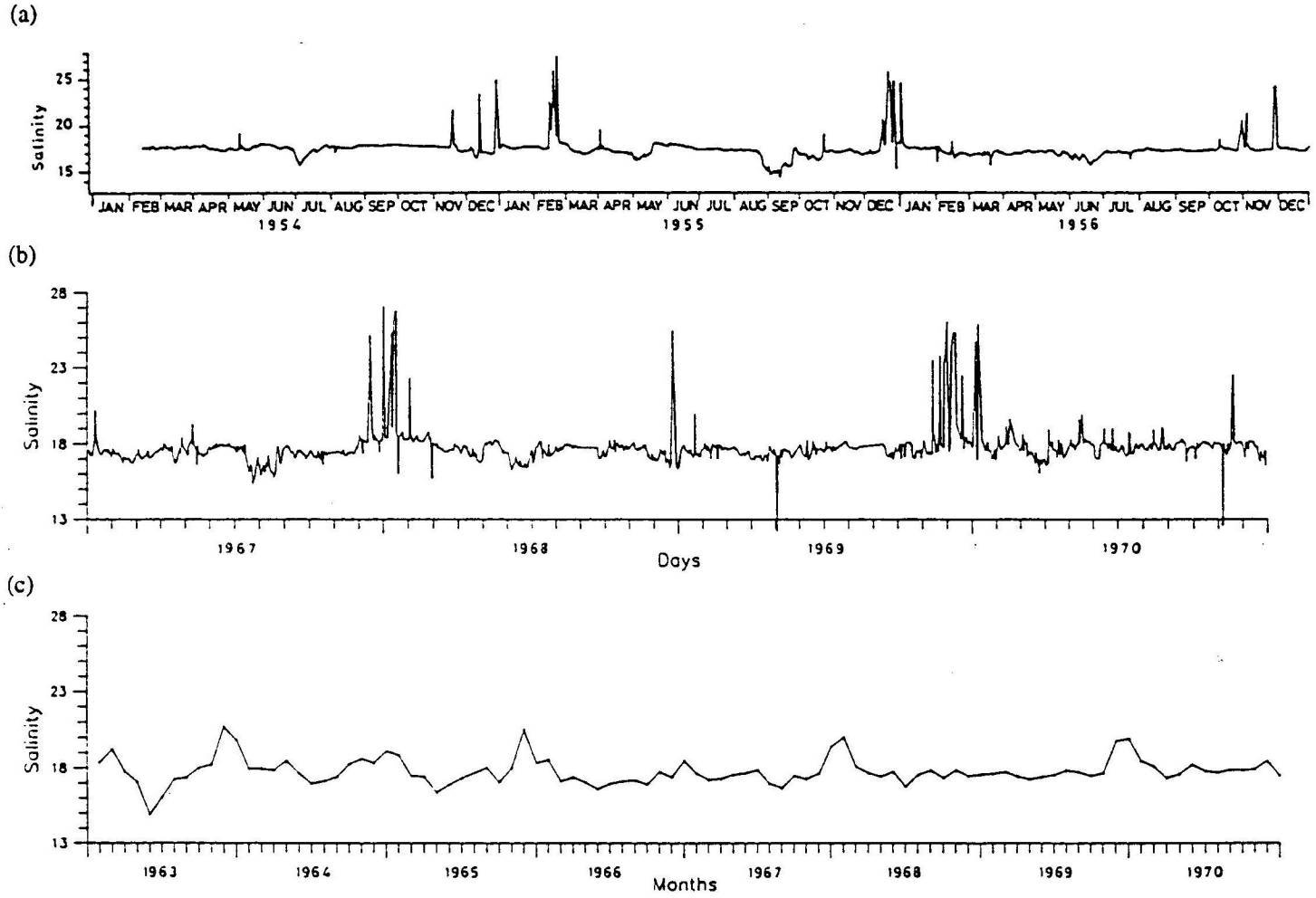

FIG.4. Time series of salinity within the Bosphorus: (a) daily measurements, 1954-1956 (redrawn after ACARA, 1958), (b) daily measurements, 1967-1970, (c) monthly averages of daily measurements, 1963-1970 (after ARTÜZ and UGUZ, 1976).

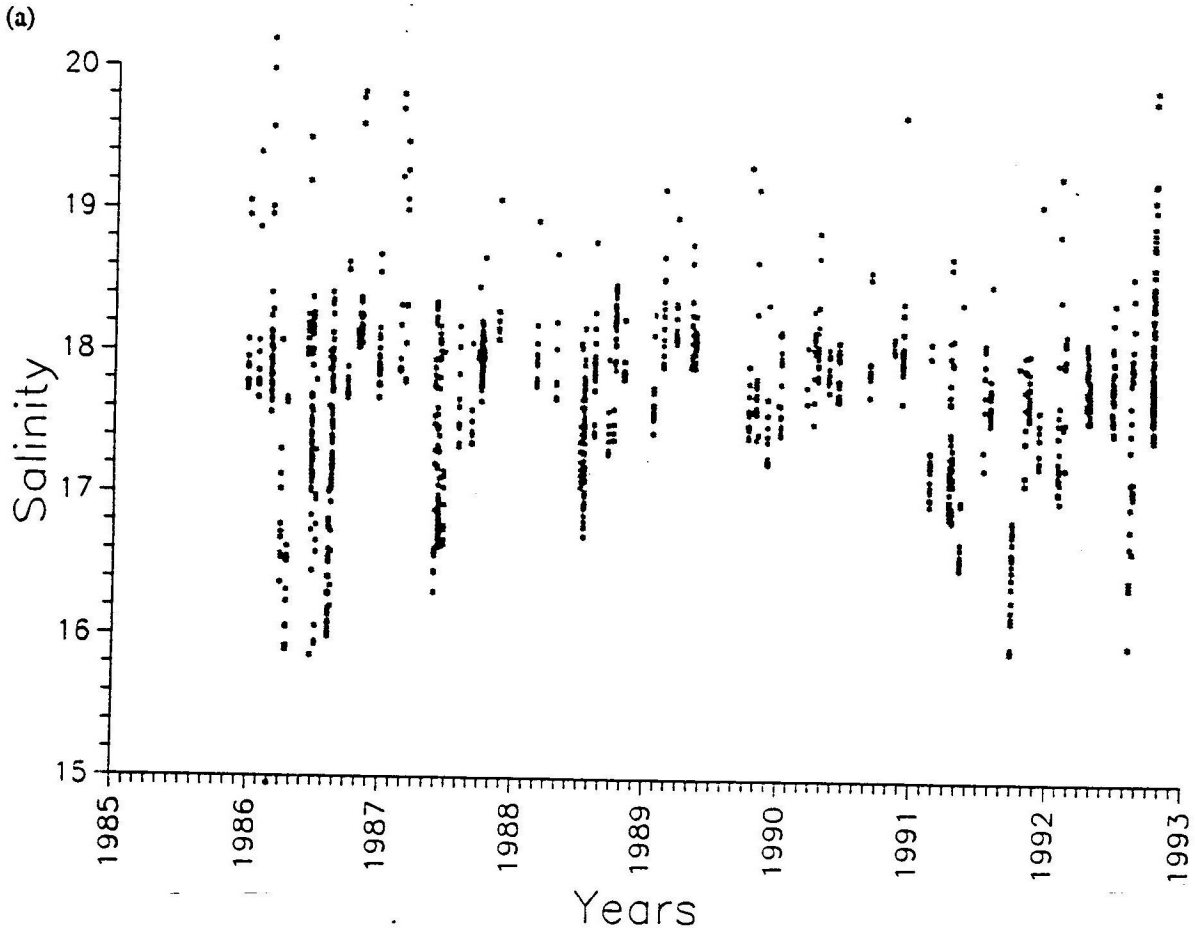

FIG.5. Surface salinity measurements (upper 10m average) in the southwestern Black Sea (between 28° and 32°E, and 41° and 42°N). Each data point corresponds to a hydrographic station occupied in the area, including the many measurements made in the Bosphorus. Time dependence with respect to (a) annual and (b, overleaf) seasonal time axes are shown separately to emphasize the different times of salinity minima in the spring-summer periods.

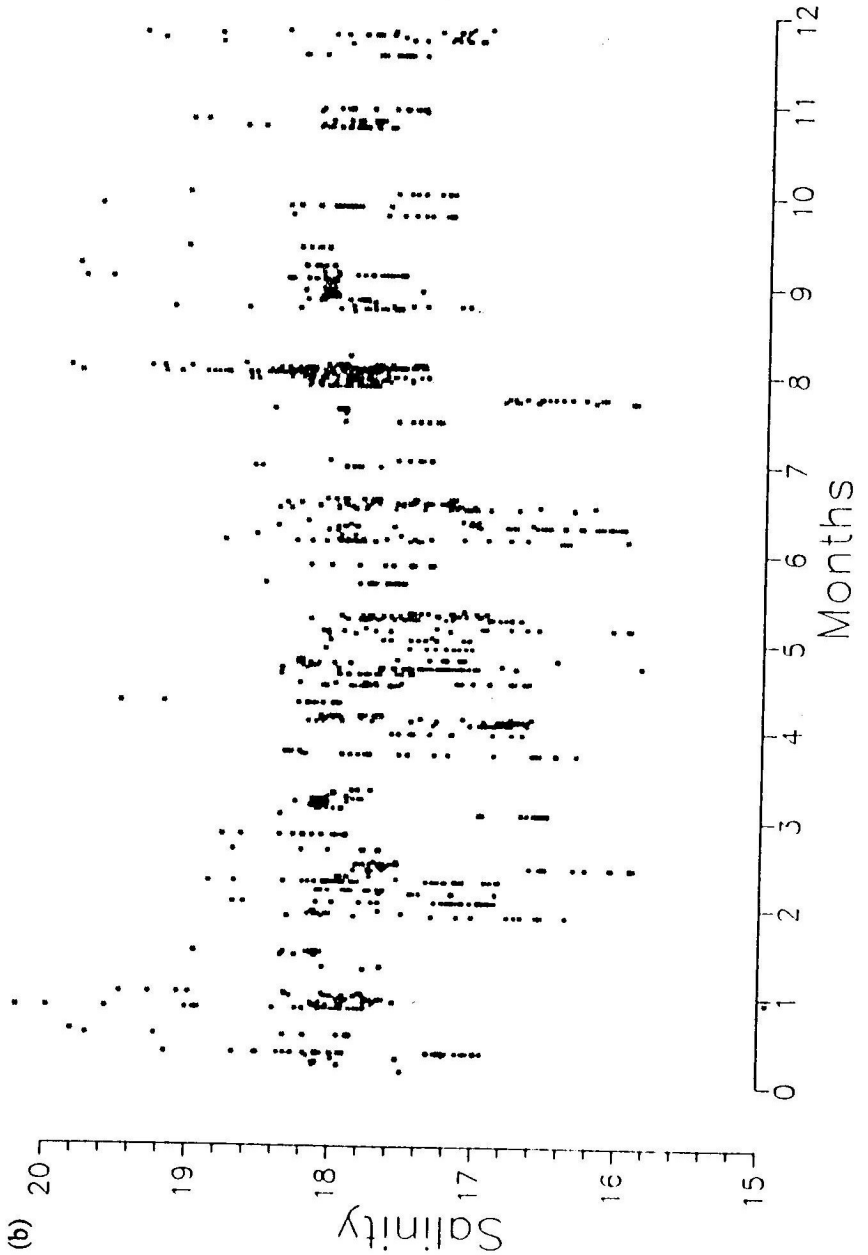
(b)
Salinity
20
19
18
17
16
15
Months
0
1
2
3
4
5
6
7
8
9
10
11
12

Fed by a rich supply of nutrients, the Black Sea is known to be a region of moderate to high productivity (KOBLENTZ-MISHKE, VOLKOVINSKY and KABANOVA 1970), compared with other parts of the world ocean. In the past (before the last decade), the peaks in primary productivity of the Black Sea were known to occur twice a year, with a major bloom mainly of diatoms (several species of *Chaetoceros*) in early spring, followed by a secondary bloom mainly of coccolithophorids in autumn (SOROKIN, 1983). Occasional blooms of coccoliths and dinoflagellates occurred mainly in coastal areas. Recently, additional summer blooms with predominance of dinoflagellates and coccoliths (*Emiliana huxleyi*) have increased in occurrence to become common in the region (BOLOGA, 1986; BENLI, 1987; HAY and HONJO, 1989; HAY, HONJO, KEMPE, ITEKKOT, DEGENS, KONUK and IZDAR, 1990; HAY, ARTHUR, DEAN and NEFF (1991). In addition, SOROKIN (1983) first reported the spring and summer development of red tides in the eutrophic waters of the western shelf. Massive red tides have been created along the Romanian and Bulgarian coasts by dinoflagellates (mainly *Exuviaella cordata*, as well as *Prorocentrum micans*, SUKHANOVA, FLING, HIBAUM, KARAMFILOV, KOPYLOV, MATVEEVA, RAT'KOVA and SAZHIN, 1988, and references cited therein) and by ciliate infusoria (*Mesodinium rubrum*, TUMANTSEVA, 1985).

Not much is known about the winter productivity, which should be expected to follow convection events bringing nutrients up from the halocline into the upper layers. SOROKIN (1983) indicates a late winter - early spring (February-March) bloom comprised of sub-arctic species with a biomass even larger than the spring-autumn blooms, but he notes that the existing sampling, mainly carried out during the good weather season may have missed the peak winter primary production. On the other hand, most winter measurements were obtained in the offshore waters; the available observations within the northwest shelf zone either do not indicate winter blooms or seem to have missed the winter peak of production (M.E. VINOGRADOV, personal communication). Our limited winter observations during February 1990 (UYSAL, 1993) indicate a massive explosion of plankton, mainly *Chaetoceros sp.* along the west Anatolian coast (see Section 4.4).

The maximum spring-autumn primary productivity (60% of the Black Sea production) is found in the northwest shelf where 87% of the total fresh water input reaches the Black Sea from major rivers contributing large amounts of nutrients and detritus onto the shallow shelf region, reducing the surface salinity and transparency (<60% of the total incident radiation reaching below 1m depth). The maximum daily assimilated carbon in this area is estimated to be on the order of 1-2gC $m^{-2}d^{-1}$. Open sea primary productivity at the centres of the western and eastern gyres of the Black Sea are typically low (0.05-0.2gC $m^{-2}d^{-1}$). Next to the high productivity areas in the northwest shelf and the northeast regions, the highest primary productivity (0.2-0.5gC $m^{-2}d^{-1}$) is reported to occur along the Anatolian (southwestern) and Romanian (western) coasts, and extends into the central region separating the eastern and western gyres (BOLOGA, 1986).

The primary productivity measurements during the Atlantis II Cruise in March-April 1969 indicated maximum values of 2.3gC $m^{-2}d^{-1}$ near the Sakarya Canyon. High values of 0.4-2.0gC $m^{-2}d^{-1}$ were also observed when following the western shelf, along the Anatolian coast, in the central region between the eastern and western basins, and in northeastern region. More recent data in the western Black Sea in May 1982 indicates a high surface primary productivity values of 1-3.9gC $m^{-3}d^{-1}$ near the Bosphorus, and 14-153gC $m^{-3}d^{-1}$ in the Danube region, verifying the eutrophication levels (BOLOGA, 1986).

Although there are limited observations, some of the above measurements suggest the western part of the Anatolian coast is a region of relatively high productivity. The algal production rate was estimated to be in the range of 0.3-0.44gC $m^{-2}d^{-1}$ from chlorophyll *a* measurements (<1.0μg l^{-1}) of the R/V *Bilim* in September 1988 and January and April 1989 along the Anatolian coast (OGUZ, BİNGEL and TUGRUL, 1990). On the other hand, May 1986 measurements near the Sakarya Canyon seemed to indicate a spring bloom with high values of chlorophyll *a* (~1.6μg l^{-1}; GÖÇMEN, 1988).

The increased influxes of highly mineralized nutrients from major rivers (such as the Danube) draining large areas of the continent have initiated eutrophication processes in recent decades; the environmental deterioration, now on the scale of a catastrophy, is being acknowledged with an increasing sense of urgency (BOLOGA, 1986; CHIREA and GOMOIU, 1986; MEE, 1992). At present the Danube introduces 60,000t y^{-1} of total phosphorus and about 340,000t y^{-1} of total inorganic nitrogen to the Black Sea, representing large increases in the last two decades (MEE, 1992). In comparison, major Turkish rivers are estimated to contribute 1700t y^{-1} of o-PO_4 and 25,000t y^{-1} of total inorganic nitrogen, and the nutrient export versus import through the Bosphorus roughly balance each other (ÖZSOY *et al*, 1992).

The eutrophication started in the northwestern shelf area influenced by the Danube and Dniestr river mouths (TOLMAZIN, 1985), and progressed south, along the western shelf (MUSAYEVA, 1985; BOLOGA, 1986). It is now evident that the eutrophication is reaching the southwestern sector, and is in fact, creating some of the adverse changes observed in the neighboring Marmara Sea. It seems that the eutrophication increased sharply in the last decade: for example a time series of more than 1100 historical Secchi disc readings in the central parts of the Black Sea illustrate that the white disc visibility has decreased from 20m in the 1920s to about 15m until the mid-1980s; recent measurements indicate that it has decreased to 5-6m in the early 1990s (EREMEEV, VLADIMIROV and KRASHENINNIKOV, 1992). In the shelf regions, eutrophication has led to hypoxia of the bottom sediments within the oxic zone (TOLMAZIN, 1985; ZAITSEV, 1991). Significant decreases have occurred in the total stocks and species of fish, many organisms have disappeared from the region, and part of the food web has been invaded by opportunistic species imported from outside the region (ZAITSEV, 1991). In the meantime, the high productivity of the region, prized by bordering countries which were not properly alert to the impending adverse changes, resulted in a massive exploitation of the fisheries.

It has been shown that the adverse changes have not been restricted to the shelf regions alone: the nutrient distribution has changed drastically throughout the entire basin (TUGRUL, BASTÜRK, SAYDAM and YILMAZ, 1992; SAYDAM, TUGRUL, BASTÜRK and OGUZ, 1992), in spite of the stability with time of the anoxic interface relative to density surfaces. The results indicate that ammonia and silicate have been depleted in the near surface waters by increased utilization in the last few decades.

The recycling mechanisms of nutrients within the basin are not clearly identified. The major source of nutrients entering the euphotic zone is often assumed to be the reserve of nutrients in the oxic and anoxic waters below the photic zone (DEUSER, 1971; FONSELIUS, 1974; SOROKIN, 1983). On the other hand, no new nitrogen seems to reach the euphotic zone from the deep water (J.W. MURRAY, personal communication); this may be one of the peculiarities of the Black Sea, leaving the atmospheric and riverine supply as the only sources of new production.

4. RESULTS

4.1 River plumes, dipole eddies and plankton blooms

Riverine influence is easily recognised in the CZCS images such as those showing the Anatolian coast on September 19, 1980 (Figs 6a,b). The feature near 32°E is the plume of the Filyos River. We also see a separated filament of river water (possibly originating from the small Bartin and Devrekani Streams near 33°E) near Cape Kerempe. The eastward bending plumes from these perennial runoff sources extend up to 50km offshore, with a colour signature indicating terrigenous sediment and organic inputs. HAY and HONJO (1989) attributed part of the deposition in offshore

sediment traps to sediments supplied by these rivers. The properties of the wide patch with wavy edges between 29°E and 31°E contrasts with those of the river dominated features described above. Firstly, the feature is essentially confined to the shelf region west of the Sakarya Canyon (Fig.1), and does not appear to be river driven. If the material yielding the visible signal were to originate from the Sakarya River (located downstream at 30°40'E) the plume would be expected east of the mouth in response to the eastward flowing boundary currents, as for the other rivers observed in the same picture. Secondly, this patch of water displays a more uniform distribution of reflectance than the river plumes. Thirdly, its reflectance is large both with respect to particulates (Fig.6a) and pigment concentration (Fig.6b), indicating that this feature is likely to be a coccolithophore bloom. We also note other patches of the same nature along the Thracian and Bulgarian coasts, which may indicate that such blooms are characteristic of the western shelf.

In Figs 7a,b (October 7, 1980) plumes originating from the Kizilirmak and Yesilirmak rivers, and from other small streams along the central Anatolian coast are observed to bend eastwards as a result of the boundary current system, and to form small eddies in the adjoining bays (east of Cape İnce, Cape Bafra and Cape Çalti). As with Figs 6a,b we note a clear predominance of inorganic particulates. The pigment calculations in Fig.7b depend on information from different bands of visible light, including some contribution of channel 3 reflectance. Yet the pigment signal of the plumes, partly associated with river-borne organics (e.g. plant debris and yellow substance) is typically smaller than the particulate signal.

In Fig.8a (October 13, 1980) the plume at the mouth of Filyos River has become weaker as a result of decreased runoff during autumn. Note that the plume from the Sakarya River, a relatively large river compared to Filyos, has very narrow coastal influence during the autumn period reviewed. This is because it drains the dry interior region, whereas the Filyos receives its water from the north Anatolian mountains, which continue to receive rainfall throughout the summer and autumn.

A mushroom eddy is visible in Fig.8a, offshore of the mouth of the Kizihrmak river at Cape Bafra. In the enlarged image of the Anatolian coast (Fig.8b) specific features can be observed. The antisymmetric spiral pattern of the tracer field trapped in the doublet, and the pattern of streamers surrounding the eddies are remarkably similar to the patterns generated in laboratory simulations.

Similar coherent structures of dipole eddies have been reproduced in laboratory experiments with rotating/stratified (FEDOROV, GINSBURG and KOSTIANOY, 1989) or stratified flows (VAN HEIJST and FLOR, 1989; VOROPAYEV, 1989). Nonlinear advective dynamics and two-dimensional dipole eddies from the collapse of impulsively generated three-dimensional flows. For example, FEDOROV and GINSBURG (1989) and FEDOROV, GINSBURG and KOSTIANOY, (1989) view dipole structures to be the universal reaction of a rotating fluid to an impulse applied to it. The momentum impulse could result from local dynamical instabilities, local winds, or river discharges. During initial development, the dipoles are often assymmetric or immature, but when a surface tracer is present (for example, sea surface temperature, biota, sediments, sea-ice), the basic surface signature of a dipole eddy is a mushroom-like pattern. Numerical studies by MIED, MCWILLIAMS and LINDEMANN (1991) confirm generation by a localized pulse; advection by the dipole velocity field then leads to a mushroom pattern in tracer fields. Dipole eddies are also the most common structures resulting from the instability of boundary currents (cf Section 4.2). For example, some laboratory experiments (GRIFFITHS and LINDEN, 1981) indicate that when long waves generated by the instability of a boundary current break, they form cyclonic/anticyclonic vortex pairs or dipoles.

The tracer pattern in Fig.8b appears mainly related to river sediments, as well as some pigments (weaker, not shown) carried by river water. The mushroom feature consists of equal sized cyclonic

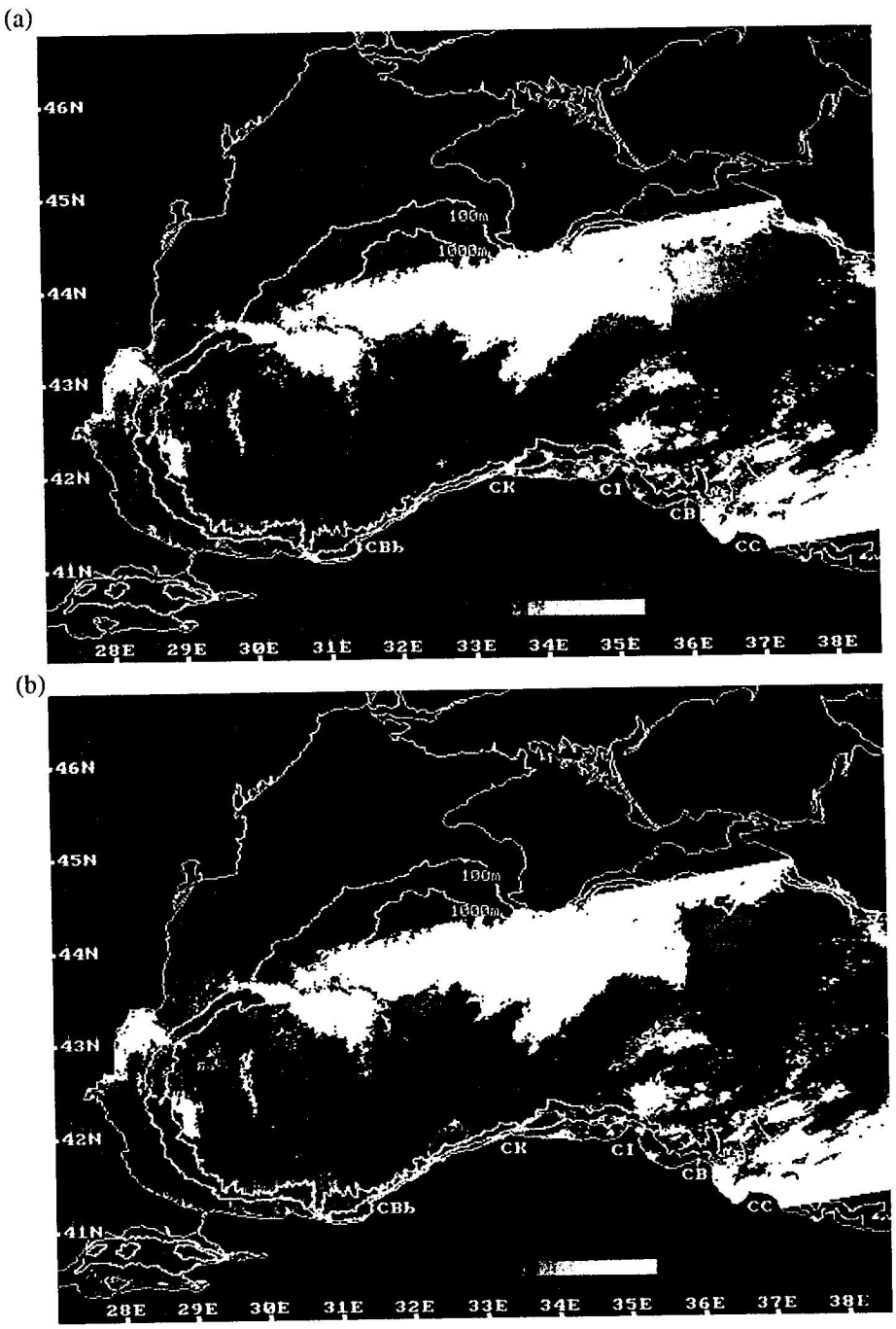

FIG.6. Coastal Zone Colour Scanner (CZCS) satellite images on September 19, 1980 showing the plumes of the Filyos and the other small rivers, and a bloom of coccolithophores on the southwestern shelf. The images represent the atmospherically corrected (a) channel 3 (550nm), (b) the calculated pigment concentration. Abbreviations used: CBb:Cape Baba, CK:Cape Kerempe, CI:Cape İnce, CB:Cape Bafra, CC:Cape Çalti.

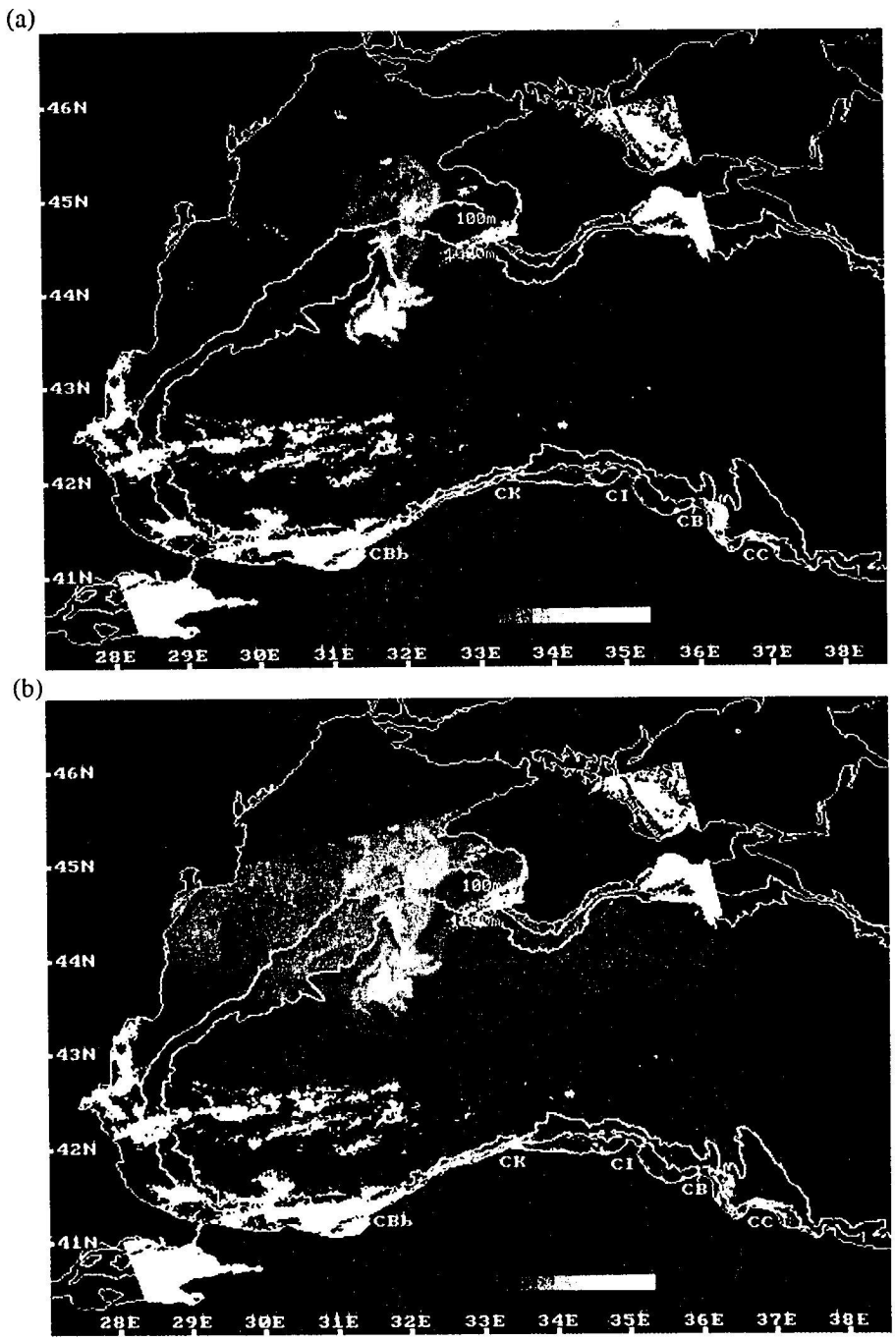

FIG.7. Coastal Zone Colour Scanner (CZCS) satellite images on October 7, 1980. The images represent the atmospherically corrected (a) channel 3 (550nm) and (b) the pigment concentration showing development of flow and associated sediment along the southwestern coast of the Black Sea, and a distinct offshore plume of Dnepr, Bug, and Dnestr Rivers.

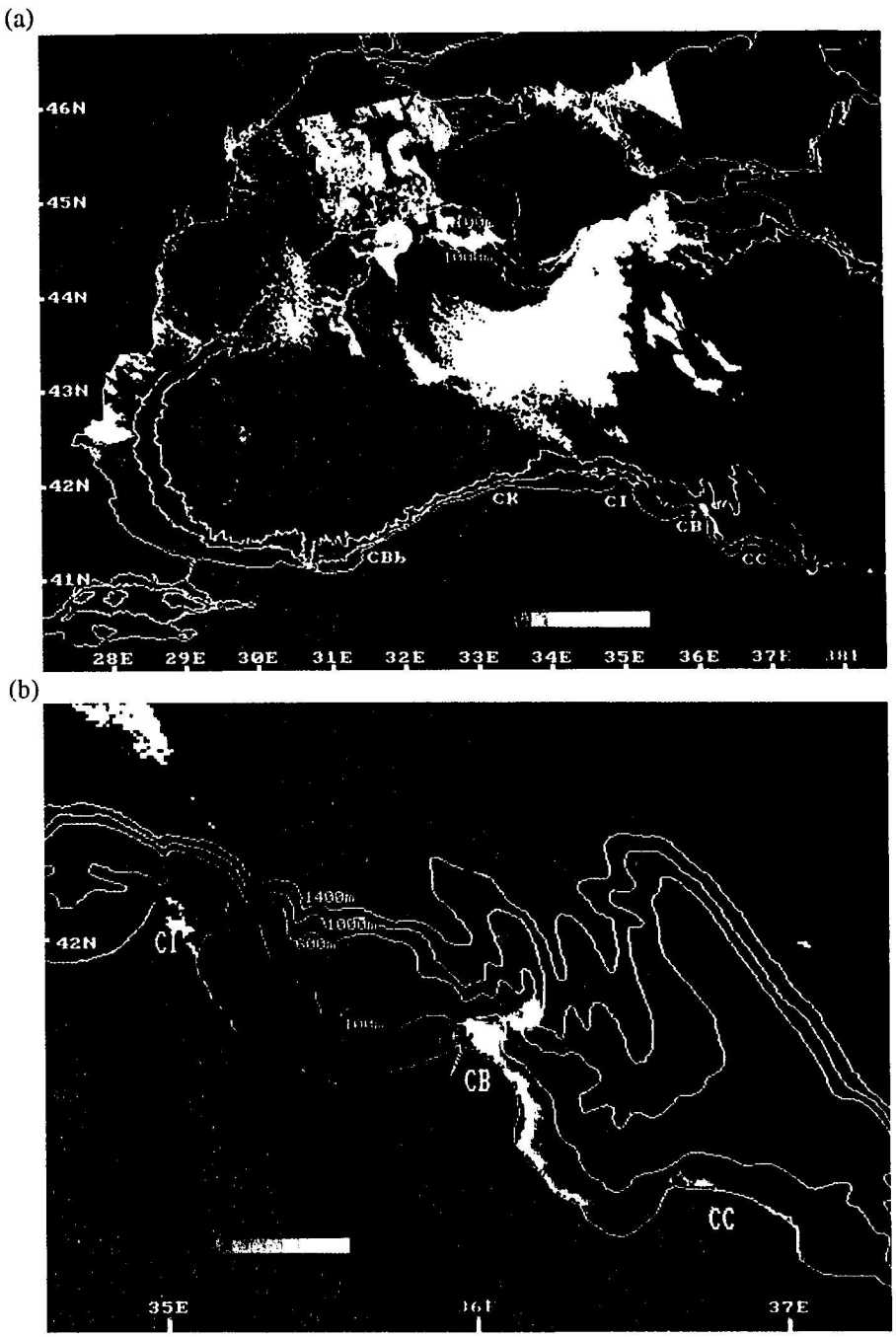

FIG.8. (a) Coastal Zone Colour Scanner (CZCS) satellite image on October 13, 1980, showing the massive plankton bloom in the northeast sector and unstable filaments near Cape Kerempe, and (b) its enlarged form showing a dipole eddy near the mouth of the Kizilirmak river. Both images are the atmospherically corrected channel 3 (550nm) of the CZCS.

and anticyclonic eddies, extending 60km offshore, and connected to the coast by a filament (the river plume) that seems to follow the depth contours of the local canyon topography adjacent to the Arhangelsky Ridge (Figs 1 and 8b). This topographic control is surprising since we suspect the flow to be confined in the surface layers. The dipole vortex could be an unstable feature generated by a pulse of momentum imparted by local winds, the river plume itself, or instabilities of the boundary current. Support for the instability hypothesis is given by similar features observed not far from the dipole: a number of filaments extending offshore from the coast near Cape Kerempe suggest an instability of the boundary current flowing along this coast.

In addition to the effects of Anatolian rivers displayed in Figs 7 and 8, a massive plankton bloom originating from the northwestern shelf can be identified. The bloom appears in both the particulate (Fig.7a) and calculated pigment (Fig.7b) fields. The high pigment concentration could well correspond to an *Emiliania huxleyi* bloom, since high spectral reflectance is obtained in all visible CZCS channels, which is characteristic of these organisms (HOLLIGAN, VIOLLIER, HARBOUR, CAMUS and CHAMPAGNE-PHILIPPE, 1983). Note that the bloom extends south from the shelf, reaching the middle of the basin, in spite of the minimum river discharges (Fig.3) expected during this season. This may suggest either the influence of northerly winds or the bloom to be independent of the size of the river plume. Investigating more closely, we see that the pigment distribution covers the entire northwest sector of the basin (Fig.7b), but the particulate signal (Fig.7a) is more confined to the region northwest of Crimea. This spectral pattern may indicate species differentiation between the shelf and open ocean plankton blooms. Only 6 days later, on October 13, 1980 (Fig.8a), the plankton bloom in the northeastern sector has become larger in size, and more complicated in texture.

Earlier during the same year, a summer plankton bloom was in progress, identified in Figs 9-13. The summer bloom originated over the northern shelf and then extended into part of the interior and across the entire western shelf region. We only discuss the northwestern sector in this section; the Danubian influence and transport in the southwest region are discussed in Section 4.2.

In Fig.10a-d different bands of the CZCS are shown for June 12, 1980, about 4 months before the data of Fig.6 were collected. The visible channel 1 data show a dark band covering the entire western shelf (Fig.1), indicating absorbance of sunlight by chlorophyll *a*, i.e. a massive bloom limited to the shelf. We note that the darkest region occurs in the northwest shelf near the Danube, where the production, under direct influence of the riverine nutrient supply, is largest. Channel 3 of the CZCS in Fig.10b indicates particulate material in the same area, and the pigment distribution in Fig.10c combined with the information given by Figs 10a and b, indicate that the particulates are mainly phytoplankton. Finally, the thermal infra-red image in Fig.10d shows a band of shelf water that is warmer than the interior, outlining the convergence region where warm surface water accumulates at the coast in agreement with the cyclonic basin circulation.

The visible data of Fig.10 can be used for the identification of multiple species of plankton. Light absorption (darker tones) in Channel 1 is maximum in the northwestern shelf region near the mouth of the Danube, with decreasing values observed along the entire western shelf (Fig.10a). In principle this maximum of absorption could result from chlorophyll *a* supported by the uniform pigment distribution in Fig.10c. In contrast to this region of absorbance, a region of Channel 1 reflectance (lighter tone) is identified at the front separating the shelf water from the interior. The frontal region is most likely populated with *E. huxleyi* as confirmed by high reflectance in the other visible bands (Figs 10a-c). As a result of the above discussion, we distinguish two populations of plankton, one occupying the western shelf region and the other populating the outer edge of the first group in the offshore frontal region. The nitrogen to phosphorus ratio of the Danube discharge determines the strength of summer phytoplankton blooms (D. AUBREY, personal communication). Particularly in June 1980, favourable N:P ratios were found in the immediate neighbourhood of the discharge,

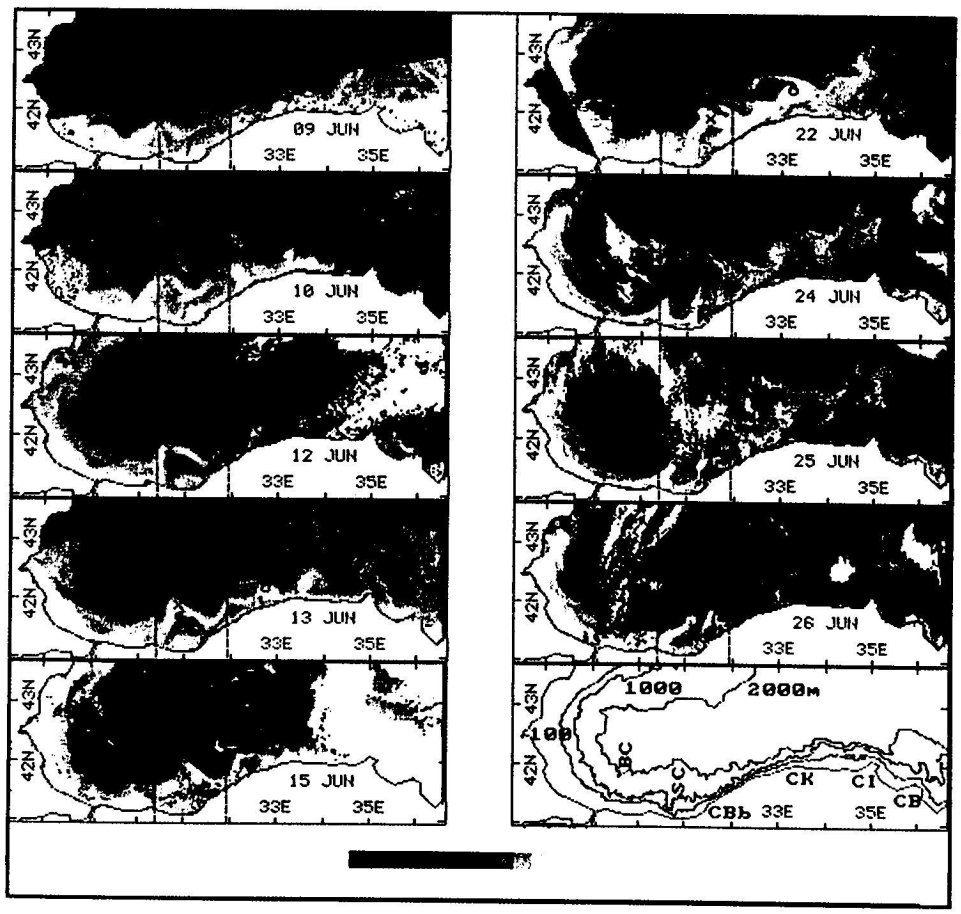

FIG.9. A sequence of CZCS channel 3 (550nm) images showing the development of the motions along the Turkish coast for the period 9 June through 26 June 1980. Abbreviations used: BC:Bosphorus Canyon, SC:Sakarya Canyon, CBb: Cape Baba, CK: Cape Kerempe, CI:Cape Ince, CB:Cape Bafra.

decreasing rapidly along the coast as a result of phytoplankton consumption.

Three days later (Figs 11a,b) we observe that the frontal region occupied by *E. huxleyi* has become unstable, and is ejecting a large filament (size ~150km) from the northwest shelf region into the interior. Note that the core of this filament contains chlorophyll *a* (Channel 1 absorption), encapsulated by high spectral reflectance species on the periphery of the filament. In Figs 11a,b and 12a,b, observed 10 and 13 days respectively after the initial image of Figs 9a-d, the filament has retained its identity, but a dipole eddy (with a better defined cyclonic member) has developed near its cap. We also note that the filament on these last two images does not seem to contain a core of visible light absorption at Channel 1; rather the entire filament becomes a region of high spectral reflectance. Also note that the area of Channel 1 absorption which initially covered the entire northwest shelf and extended south partially to cover the western shelf, has become smaller and more confined to the Danube mouth in the later images.

The above observations seem to suggest there is competition between the shelf species and the

coccolithophore bloom on its periphery. Initially the high reflectance species at the shelf edge forms a contrast with the other species distributed in the shelf region. In the sequence of following images, the shelf species are observed to become more confined, and the high reflectance species dominates the entire region excluding the vicinity of river mouths. The observed features suggest segregation behaviour (e.g. OKUBO, 1980) typically encountered between similar but competing species.

4.2 A time series study of meandering flow and primary production along the Anatolian coast

In addition to the other aspects discussed above, outstanding dynamical processes of shelf-open ocean interaction, with important impact on productivity are investigated in Figs 9-13. The open ocean production activity of a filament originating from the northwestern region has been revealed above. Similarly, a unique pattern of meandering currents along the Anatolian coast with efficient dispersion result in a massive plankton bloom in that region.

The fields derived from the CZCS serve as tracer fields visualizing the motions transporting them. The motion along the Anatolian coast basically consists of a pattern of eastward propagating waves with an embedded train of mesoscale eddies. The series of images in Fig.9 are used to calculate (by following points with fixed phase) an eastward propagation speed of 10-15cm s^{-1} ($\cong$10-15km d^{-1}) for the meandering motion. Based on a review of several images used in their study, OGUZ *et al*, (1992) claimed that they had not been able to detect any translation of features along the boundaries, and suggested that the translation speeds could be too small to be detectable. In the present case, we find noticeably fast propagation of wave motions superimposed on mean boundary currents.

There is close correlation of the flow features with the continental slope topography. The eastward propagating oscillatory motions are generated at the abrupt termination of the western continental shelf at Sakarya Canyon. As the whole pattern moves east in Fig.9 and in Figs 10-13, the eastern terminus of the shelf region appears as the generation region for the wave motion. The uniform distribution of tracers observed along the western shelf, e.g. in Figs 10b,c, verifies uniform flow of the cyclonic boundary current. This uniform flow in the west is replaced by undulating features east of Sakarya Canyon.

During early development (Fig.10) the wave pattern is regular, though filaments with offshore extensions are visible near Cape Kerempe. Ten days later (Figs 9 and 12), the meander has developed into a train of cyclonic and anticyclonic regions with a complex pattern of filaments extending offshore. In fact, the overall appearance of the motion in Fig.12 is reminiscent of a turbulent jet flow, with a core containing numerous meanders and filaments. This jet follows the 30° (from east) oriented western Anatolian coast from Sakarya Canyon to Cape Kerempe, where it begins to separate from the coast, and becomes more complex to the east. Note that this is also the region where the steep bottom topography adjacent to the coast is replaced by a wide continental shelf extending from Cape Kerempe to Cape Bafra.

In Fig.13, only 3 days after the image in Fig.12, we observe that the jet flow that developed earlier has widened and become totally separated from the coast east of Cape Kerempe. The wide jet terminates with a dipole-like cap extending to the mid-basin region east of Cape Ince. In this fully developed state, we observe numerous cyclonic and anticyclonic eddies within the turbulent jet. (Note that this particular image has also been used by MURRAY and IZDAR, 1989, and on the cover of MURRAY, 1991).

Also note the rapidity of the development observed in Figs 9-13: in merely two weeks, an entire

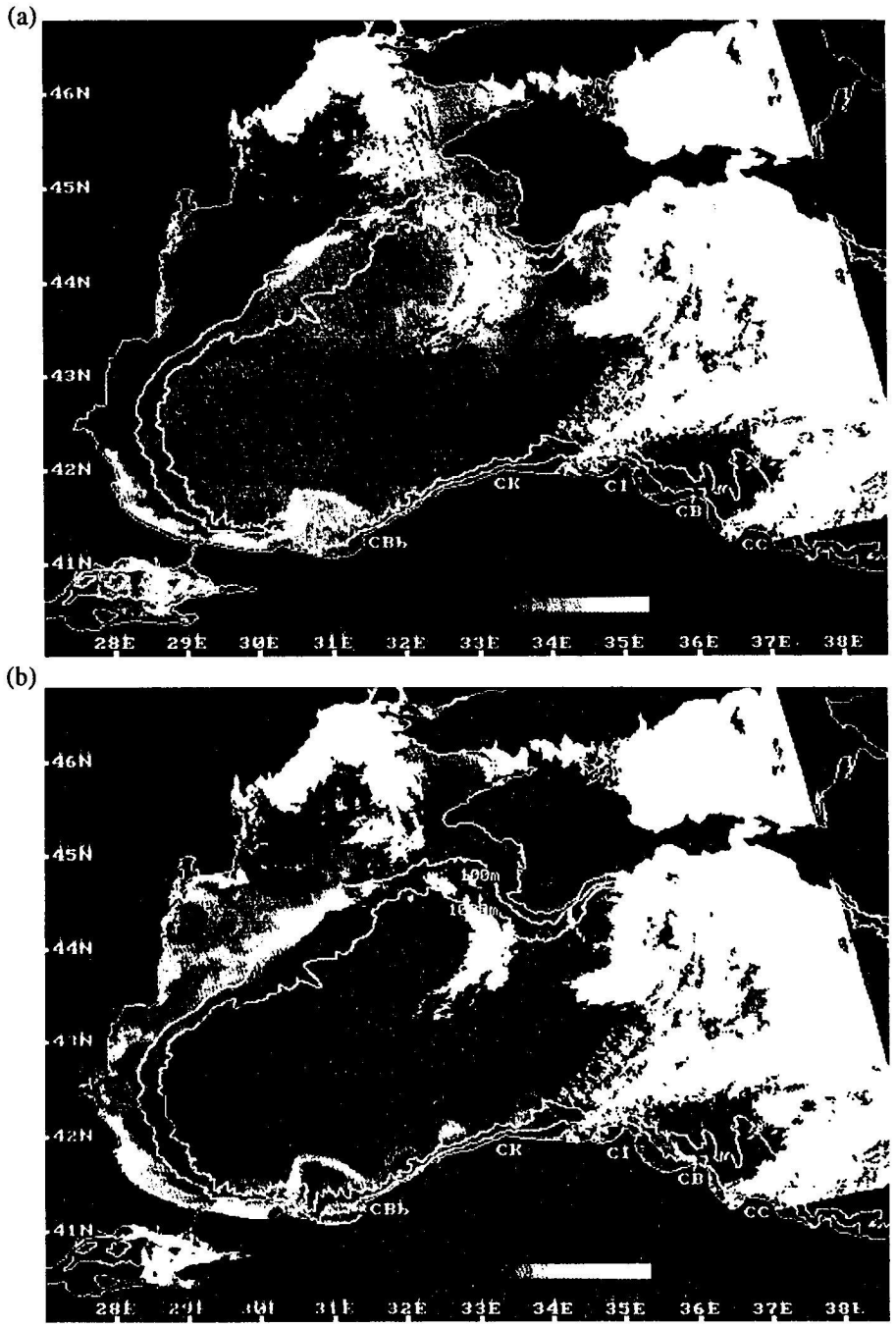

FIG.10. Coastal Zone Colour Scanner (CZCS) satellite images on June 12, 1980. The images represent the atmospherically corrected (a) channel 1 (443nm), (b) channel 3 (550nm), (c) the calculated pigment concentration and (d) thermal infra-red channel, showing development of flow and associated primary productivity along the west and southwestern coast of the Black Sea. (In this and the following thermal images, the darker tones represent warmer and the lighter tones represent colder water.)

(c)

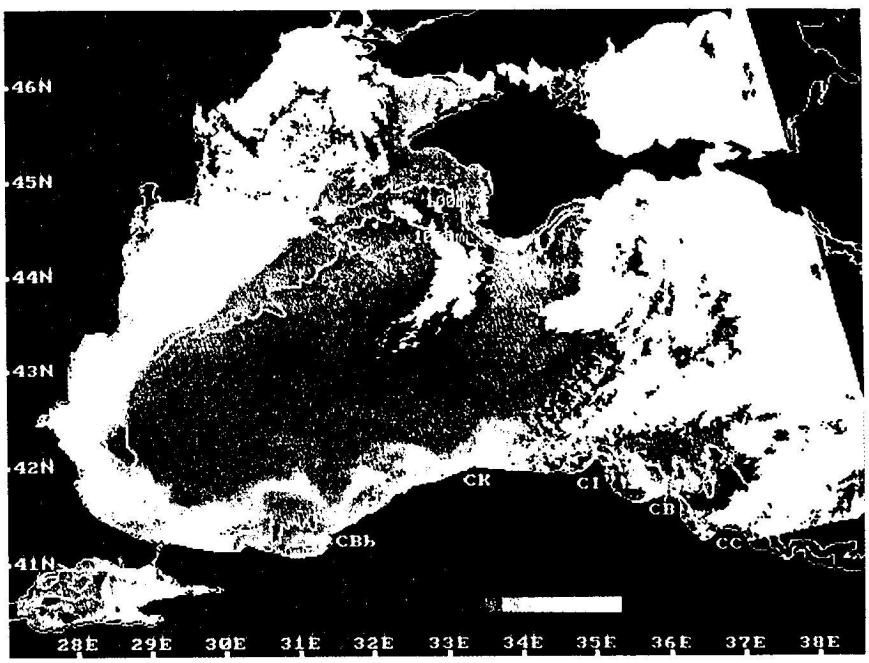
46N
45N
44N
43N
42N
41N
28E
29E
30E
31E
32E
33E
34E
35E
36E
37E
38E
CK
CI
CB
CC
CBb

(d)

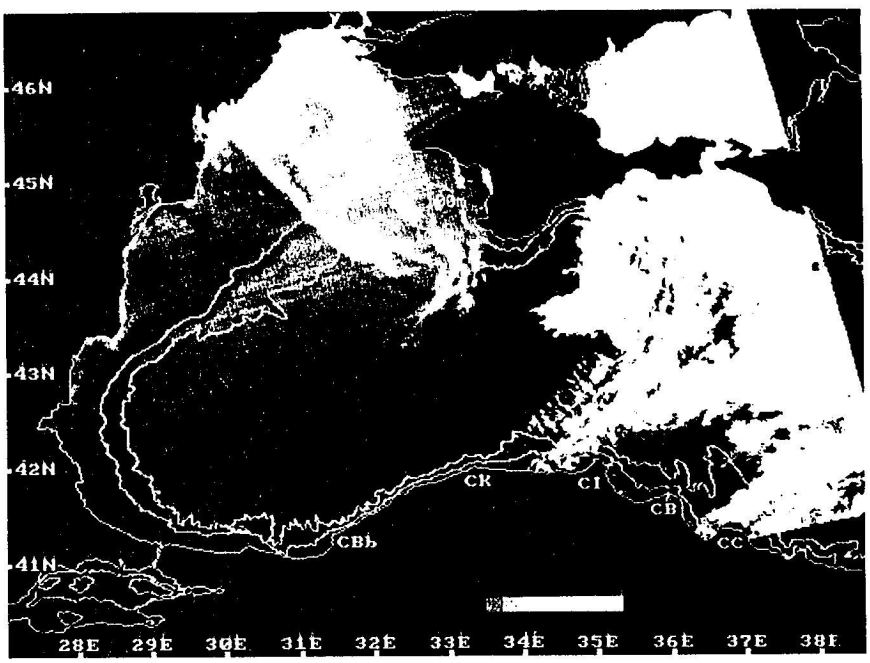
46N
45N
44N
43N
42N
41N
28E
29E
30E
31E
32E
33E
34E
35E
36E
37E
38E
CK
CI
CB
CC
CBb

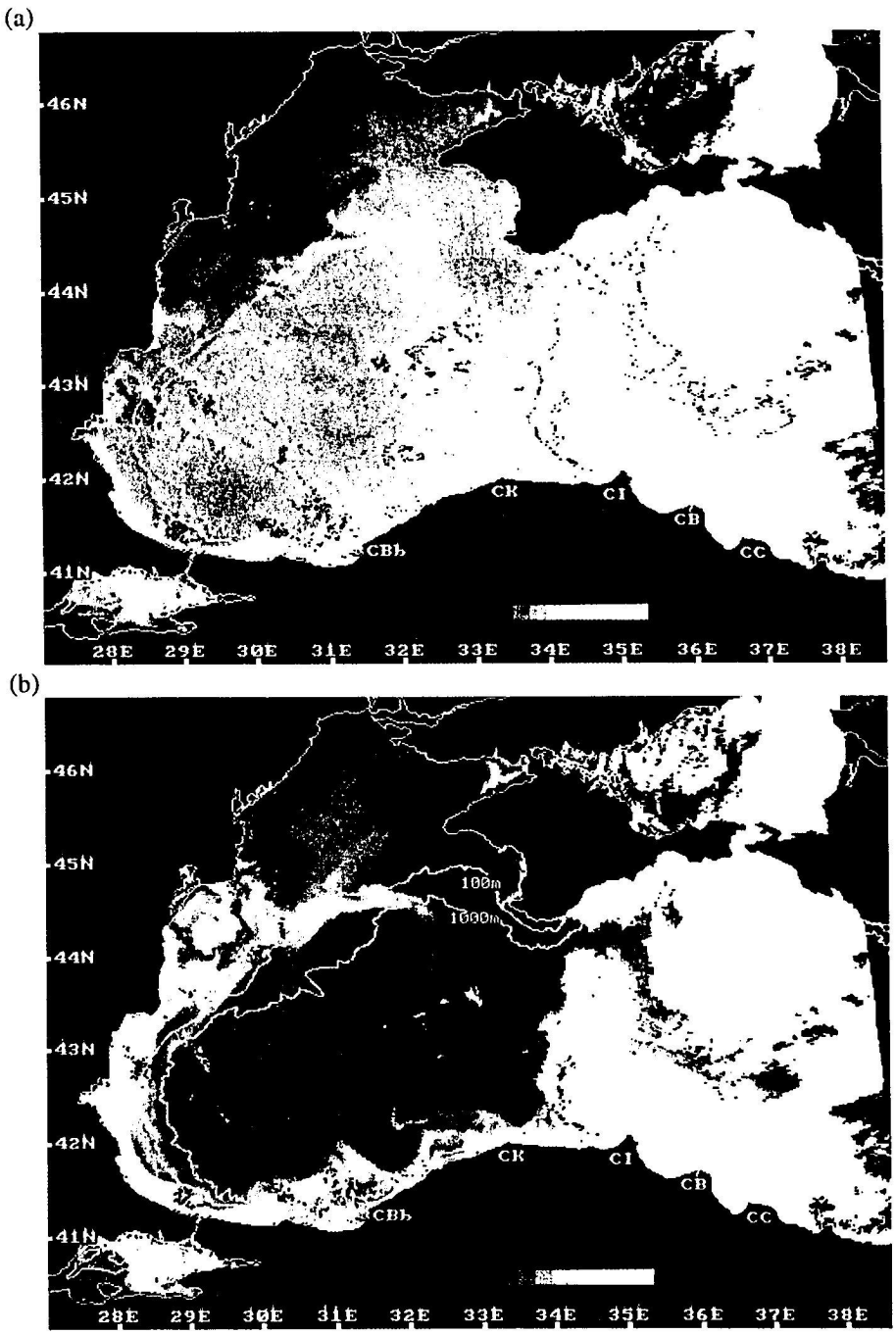

FIG.11. Coastal Zone Colour Scanner (CZCS) satellite images on June 15, 1980. The images represent the atmospherically corrected (a) channel 1 (443nm), (b) channel 3 (550nm) showing development of flow and associated primary productivity along the west and southwestern coast of the Black Sea.

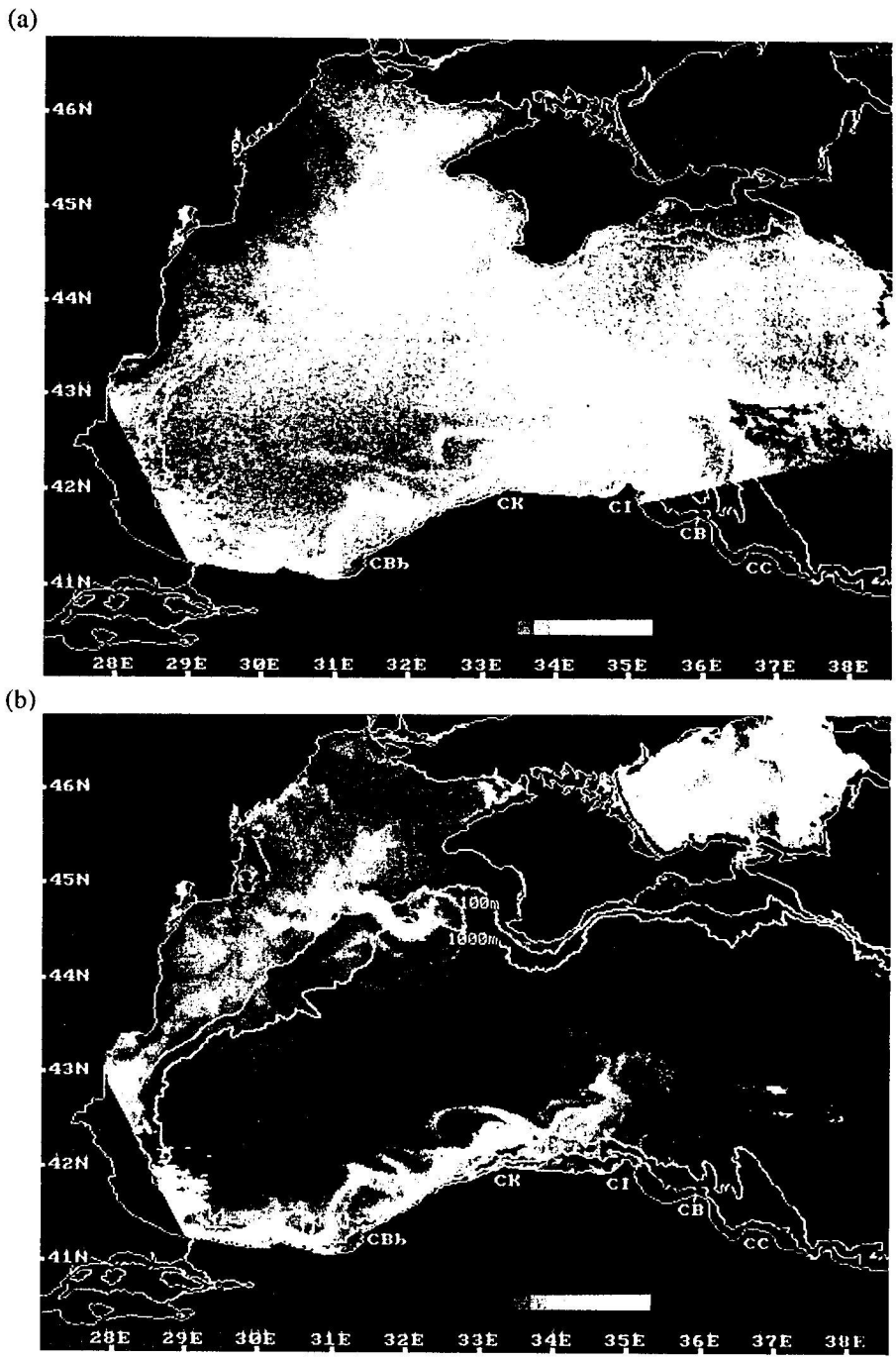

FIG.12. Coastal Zone Colour Scanner (CZCS) satellite images on June 22, 1980. The images represent the atmospherically corrected (a) channel 1 (443nm), (b) channel 3 (550nm) showing development of flow and associated primary productivity along the west and southwestern coast of the Black Sea.

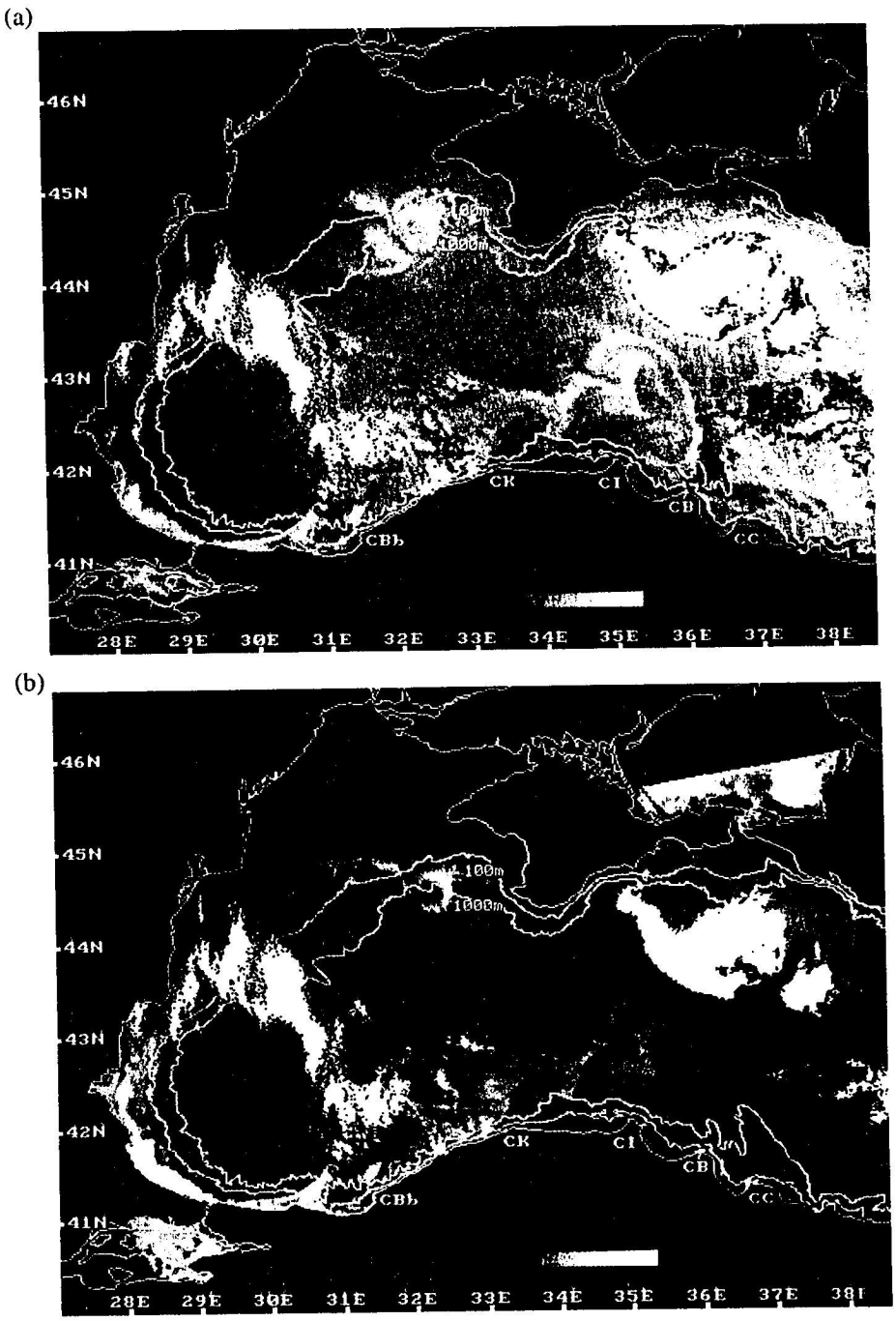

FIG.13. Coastal Zone Colour Scanner (CZCS) satellite images on June 25, 1980. The images represent the atmospherically corrected (a) channel 1 (443nm), (b) channel 3 (550nm) showing development of flow and associated primary productivity along the west and southwestern coast of the Black Sea.

current system has become modified in character, and unstable eddies and filaments have developed within time scales of a few days. This is in marked contrast with the circulation dynamics in the neighbouring regions, for example in the Levantine Basin of the Eastern Mediterranean Sea (e.g. ÖZSOY, HECHT, ÜNLÜATA, BRENNER, OGUZ, BISHOP, LATIF and ROZENTRAUB, 1991), where long-term persistence is a basic property of coherent structures. This comparison reveals the roles of strong ambient stratification and of lateral sources of buoyancy in supporting unstable motions in the Black Sea environment.

Baroclinic instability is the mechanism most frequently used (numerous examples given in Section 1) to explain unstable motions in buoyant coastal flows. Although we oberve that the meandering motion of the west Anatolian boundary current is triggered by a discontinuity in shelf topography, baroclinic instability appears to contribute to its subsequent growth. Instability of fronts leading to large meanders, bores or breaking waves was examined by STERN (1980). It is these motions that lead to exchanges across the front, as indicated by the large excursions in Figs 9-13. It is noticeable from the increasing sizes of the eddies that significant entrainment is taking place.

Baroclinic instability could be one of the most relevant mechanisms generating time-dependent motions along frontal regions. Realistic boundary flows with horizontal density gradients are often found to be unstable to small perturbations (e.g. MYSAK and SCHOTT, 1977; GRIFFITHS and LINDEN, 1981; IKEDA *et al*, 1984, 1989; QIU, 1988; CHAO, 1990; BECKERS and NIHOUL, 1992), and as a result the unstable waves in many cases grow into large amplitude meanders or paired coherent vortices. Laboratory experiments of CONDIE (1989) show that the energy of the unstable motions, including coalescent eddies and dipoles, is extracted from the mean flow at the Rossby deformation radius scales, and later transferred to larger scales by nonlinear processes. During the nonlinear growth stage of the instability, QIU *et al* (1988) showed that disturbances starting at the grid-scale were transformed into finite amplitude meanders with 'backward breaking' tendency, enhancing the cross-shelf exchanges. Laboratory experiments of CARSTENS *et al* (1984) indicated anomalous current loops separated from the coast. CHAO (1990) differentiated between prograde (fronts rising to the surface in the same direction as the bottom topography, e.g. Gulf Stream or upwelling fronts) and retrograde (isobaths and isopycnals slanted in opposite senses, e.g. density driven boundary currents with buoyant water near the coast, such as in the Black Sea) fronts, arguing that prograde fronts are more amenable to slanted convection (baroclinic instability) than retrograde fronts. However, it was demonstrated that enhanced meander and eddy growth could occur as a result of relaxation processes, e.g. temporally varying buoyancy forcing, which seemed to be more important in the case of retrograde fronts and more effective than the other possible forms of external forcing (such as winds or small topographic variations).

The observations also illustrate how the dynamics of the meandering jet flow along the Anatolian coast of the Black Sea is influenced by strong interactions with topography and by changes in the coastline orientation. The flow along the western shelf is most probably in a state of geostrophy, following the bathymetric contours of the shelf/slope region. Once triggered by the sudden depth change at Sakarya Canyon, the ensuing motions are unstable and, therefore, not able to readjust to a steady uniform flow along the remaining part of the coast. The jet flow becomes wider and more turbulent with distance from the step, and with time.

The mechanism of generation of the oscillatory motions by the step topography is not clearly understood. We expect oscillatory motions to be generated by the interaction of a topographic barrier with barotropic shelf/slope flows taking the coast (shallower depths) to the left in the northern hemisphere. Considering that the analogous effects of planetary vorticity gradient (β) and topography (i.e. contributions to variations in f/H, where f is the Coriolis parameter and H the depth

of the flow), we can compare flows bounded on the left hand side with eastward flows in the case with planetary vorticity gradient. Oscillatory motions are created when an eastward flowing β-plane barotropic jet crosses a step topography, while a smooth readjustment occurs for westward flowing jets (SHETYE and RATTRAY, 1982), confirming well known results of BATCHELOR (1970). The above results suggest that the western Anatolian jet flowing across the Sakarya Canyon would not be subjected to meandering or oscillatory motions if this jet were to be purely barotropic. On the other hand, SPITZ and NOF (1991) indicate that a barotropic boundary current would be forced to separate from the coast when it encounters a large step with the depth increasing downstream, regardless of the direction of flow relative to the coast.

Sudden changes in topography are expected to lead to oscillatory motions even in the case of a right hand side coast, when baroclinic modes are included. In fact, barotropic flows impinging on a step topography can be expected to generate large amplitude baroclinic motions (e.g. CUSHMAN-ROISIN and O'BRIEN, 1987). Oscillatory motions created by interacting baroclinic and barotropic components of a boundary current near canyon or ridge topographies are illustrated by HÄKKINEN (1987).

Interactions with coastline perturbations were found to create standing waves, as well as baroclinic eddies and filaments in the case of upwelling fronts (NARIMOUSA and MAXWORTHY, 1987), and to lead to meanders by pure geometrical adjustment to depth contours (without imposing baroclinic instability) in the case of ice-edge fronts (IKEDA, 1987). The role of bottom topographic features was found to augment the baroclinic instability in the case studied by IKEDA (1989). In the case of upwelling fronts, NARIMOUSA and MAXWORTHY (1985) found large stationary meanders and filaments generated by a bottom ridge. HAIDVOGEL, BECKMANN and HEDSTRÖM (1991) and HOFFMANN, HEDSTRÖM, MOISAN, HAIDVOGEL and MACKAS (1991) found offshore filaments generated by the interaction of a boundary current (upwelling front) with topographic variations. During later stages of development, the evolving filaments were shown to lead to self-advecting dipole eddies detached from the coastal region.

An important effect of topography we observe in the case of the west Anatolian boundary current is the separation of the jet from the coast at Cape Kerempe, where the flow encounters a widening shelf topography. LEAMAN and MOLINARI (1987) studied the effects of a linearly widening shelf and found that this situation can lead to vertically sheared flows perpendicular to the coast, resulting in flow separation. The change in the angle of the coastline near Cape Kerempe can be a secondary factor leading to flow separation. Laboratory studies illustrate eddy shedding and separated flows downstream of headlands (e.g. BOYER and CHEN, 1987).

Although the flow is made visible by productivity and particulate material on the western continental shelf, these tracers are neither conservative nor have uniform sources. For example, we observe changes of reflectance both along the western shelf and at the Sakarya Canyon in Figs 10a-d. In particular, sharper changes of concentration occur across the Canyon. Vertical mixing and resuspension of bottom sediments created by three dimensional motions at the edge of the Canyon (ÖZSOY *et al*, 1993), and local increases in productivity (GÖÇMEN, 1988) can contribute to these changes.

The cyclonic circulation of the Black Sea is outlined by the bio-optical properties modified along the western shelf. Much of the interior and the eastern basin have considerably smaller pigment and particulate concentrations. Note also that the satellite data in Figs 9-13 correspond to the period when the Danube discharge is maximum. Furthermore, the data of SERPOIANU *et al* (1992) (Section 3.3) suggest that 1980 was characterized by relatively high runoff and lower salinities near the Romanian coast.

HAY and HONJO (1989) examined the vertical particle flux at two sites in the southwestern Black

Sea using sediment traps during the 1982-1987 period. They observed that the dominant fraction of the annual flux was deposited during short plankton bloom periods lasting less than a month at a site 80km offshore from the Sakarya Canyon. At the other site 40km offshore from Amasra (west of Cape Kerempe), the short term fluxes were less dominant. The nearshore traps indicated *E. huxleyi* blooms in the summer, autumn and early winter, in contrast to the offshore traps where more than half of the annual particle flux was deposited during short (~one month) periods of spring/summer blooms. Some spring blooms of *E. huxleyi* were accompanied by the diatom *Rhizosolenia*.

It appears that the images in Figs 9-13 were obtained in the short period (<1 month) of an early summer bloom, during which rapid changes in the spatial distribution of species were observed, with *E. huxleyi* dominating the western basin towards the end of the observation period, excluding the near field of the Danube delta.

About 20 days later than the fully developed bloom in Fig. 13, we observe absorption at channel 1 in the Azov Sea, the northwestern shelf and along the Anatolian coast (Fig. 14a). The regions of strong absorption in channel 1 in the northwest shelf and the Azov Sea appear to delineate regional blooms of phytoplankton chlorophyll other than *E. huxleyi* (possibly dinoflagellates), characterized with high reflectance in channel 3 accompanying channel 1 absorption. The same period marks the termination of the *E. huxleyi* bloom along the Thracian and Anatolian coasts, because no colour signature of either particulates (Fig. 14b) or pigments (not shown) are present in these regions. The channel 1 absorption without any channel 3 reflectance in the patches along the Anatolian coast could be a result of flavins released into the water during bacterial production, since these dissolved chemicals can lead to absorption at 450nm (COBLE, GAGOSIAN, CODISPOTI, FRIEDERICH and CHRISTENSEN, 1991). Although the depth distribution of flavins has a maximum below the euphotic zone in the Black Sea (COBLE *et al*, 1991), eddy-induced upwelling along the central part of the Anatolian coast, as indicated by the infra-red data (Fig. 14c) may have increased their surface concentrations. The upwelling structures observed in Fig. 14c are typical of the summer months, a fact we investigate further in Section 4.3.

Note that the spreading pattern of production displayed in Figs 9-13, and confirmed by *in situ* measurements, implies that the eutrophication must have started near the Danube, proceeded south along the shelf, and finally reached the interior via cross-frontal turbulent exchanges during the early part of the last decade, when the CZCS data were obtained. It is suspected that this pattern has been significantly altered in recent years, leading to a recent decrease in the optical transparency o the surface waters even at the central regions of the Black Sea (EREMEEV *et al*, 1992), implying basin-wide intense phytoplankton blooms, confirmed by some of our recent data (not presented).

Figures 9-13 emphasize the production on the western shelf and the importance of horizontal spreading by the interactions between the shelf and deep sea regions. D. AUBREY (personal communication) has reviewed monthly averaged CZCS pigment data from 1979, 1980 and 1981 and has found the same region of influence for phytoplankton blooms with similar cross-shelf influences. In fact, he indicates a higher production in 1981 as compared to 1980 represented by our data. This higher production in 1981 seems to be a result of a Danube discharge with a high ratio of inorganic nitrogen to phosphorus (N:P), preceding the summer productivity maximum observed during that year.

Finally in this section, we note that the summer productivity in the western Black Sea shelf appears to influence the productivity in the eastern half of the Sea of Marmara. Earlier results (ÜNLÜATA and ÖZSOY , 1986; BASTÜRK, SAYDAM, SALİHOGLU and YILMAZ, 1986) suggest that the upper layer transport from the Black Sea and the entrainment/recycling of nutrients from the underlying Mediterranean water into the jet flow issuing from the Bosphorus are the main processes leading to production in the Sea of Marmara. In fact, the highest productivity in the Sea of Marmara

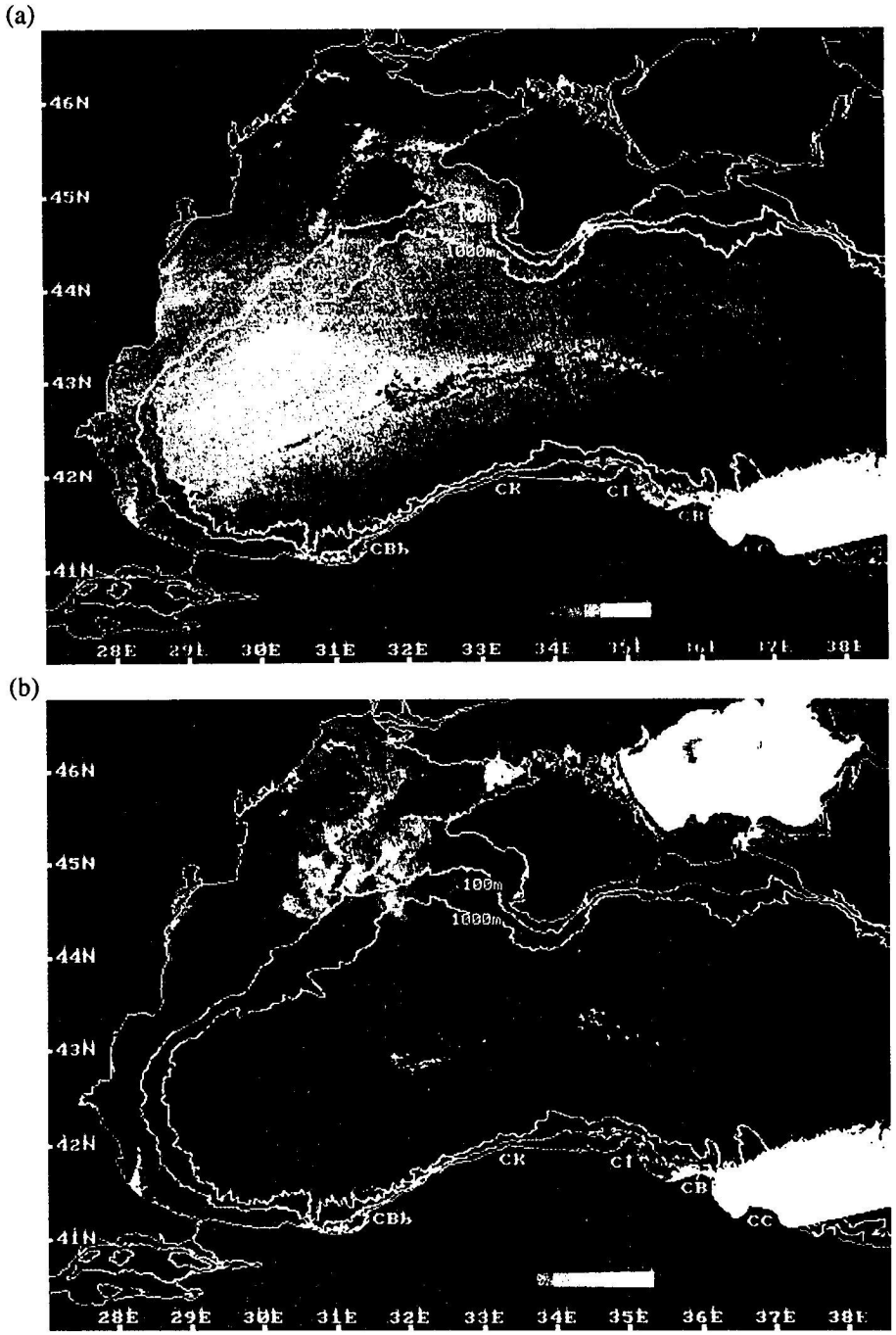

FIG. 14. Coastal Zone Colour Scanner (CZCS) satellite images on July 15, 1980. The images represent the atmospherically corrected (a) channel 1 (443nm), (b) channel 3 (550nm) and (c) thermal infrared channel, showing the phytoplankton blooms in the northwestern shelf and the Sea of Azov, simultaneously with the development of an upwelling event and post-bloom dissolved materials along the Anatolian coast.

(c)

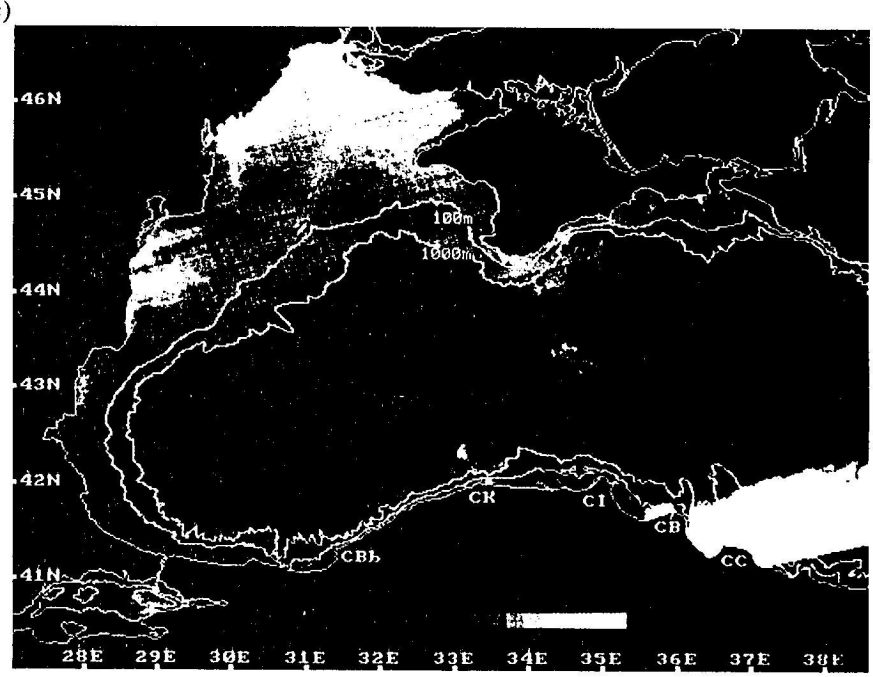

occurs in winter, when wind mixing enhances nutrient inputs into the upper layer, but secondary particle and chlorophyll maxima are found in summer, following peak discharges of the Bosphorus. A plankton bloom in the Sea of Marmara is shown in Figs 10-13 at the same time as the bloom along the shelf region in the western Black Sea. Figures 14 and 15 confirm that the intensity of the Marmara productivity subsides together with the productivity in the Black Sea. These results indicate a direct influence in summer of Black Sea surface waters transported through the Bosphorus.

4.3 Summer upwelling along the Anatolian coast

Based on a set of individual images from different years, the Anatolian coast from Cape Baba to Cape Ince can be identified as a region of upwelling starting in early summer and lasting until early fall.

Upwelling along the Anatolian coast is indicated in the CZCS thermal infra-red image of July 15, 1980 (Fig.14c). The successive images in Figs 14c and 15a-3 indicate a persistent upwelling event during the two month period of July-September 1980. It is remarkable that the upwelling event starts about one month after the period of Figs 9-13, when a cyclonic (downwelling) basin circulation with warm coastal waters (e.g. Fig.9d) was observed in the same region.

The cold water patches initially occur in the form of regular eddies in Fig.14c. Only two days later, in Fig.15a, we observe that the initial forms have been stretched in the offshore direction,

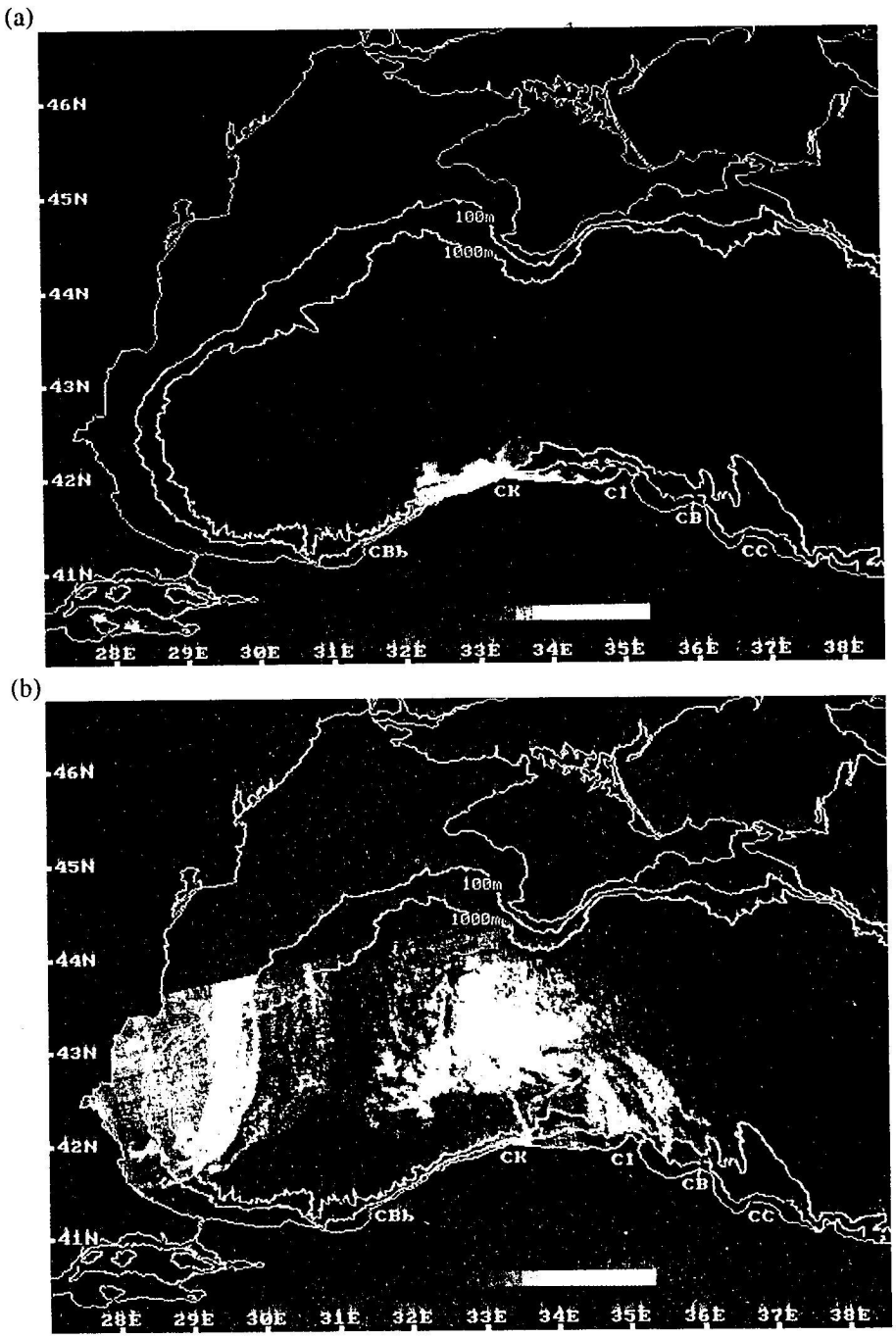

FIG. 15. Coastal Zone Colour Scanner (CZCS) satellite images on (a) July 17, (b) July 22, (c) August 29, (d) August 31, and (e) September 9 1980, representing the atmospherically corrected thermal infra-red channel.

(c)

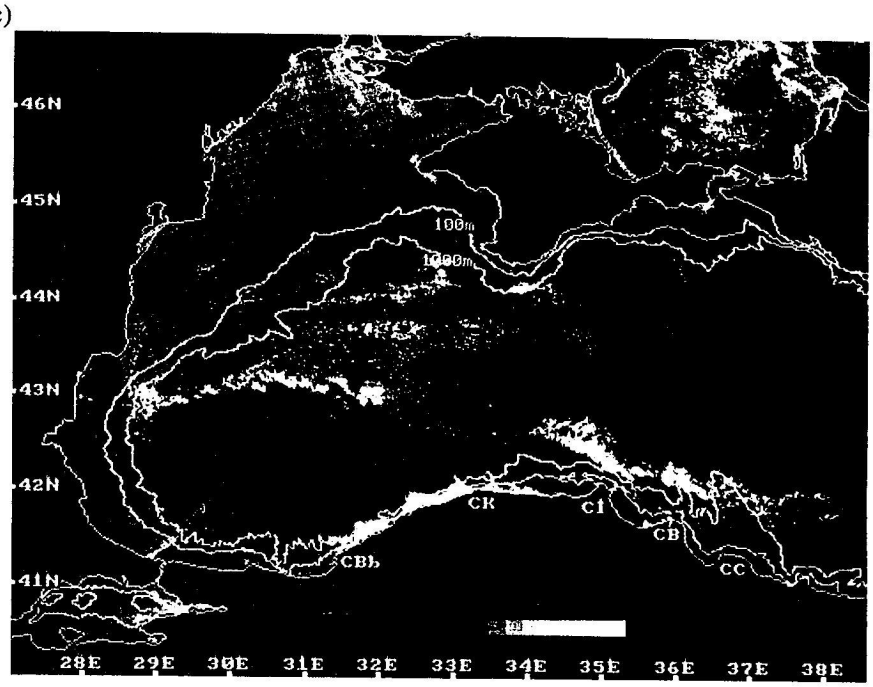
46N
45N
44N
43N
42N
41N
100m
1000m
CK
CI
CB
CC
CBb
28E 29E 30E 31E 32E 33E 34E 35E 36E 37E 38E

(d)

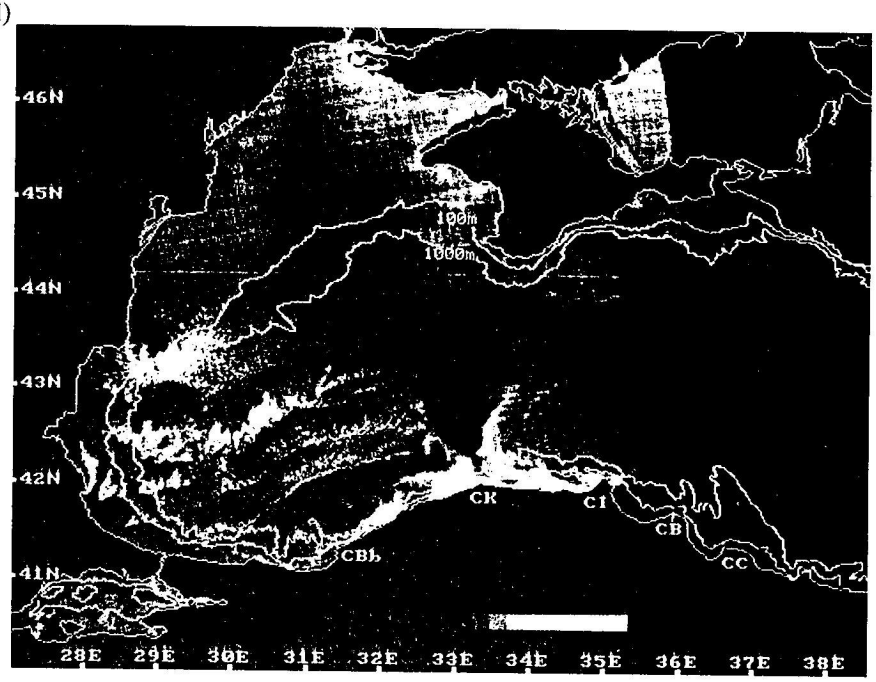
46N
45N
44N
43N
42N
41N
100m
1000m
CK
CI
CB
CC
CBb
28E 29E 30E 31E 32E 33E 34E 35E 36E 37E 38E

(e)

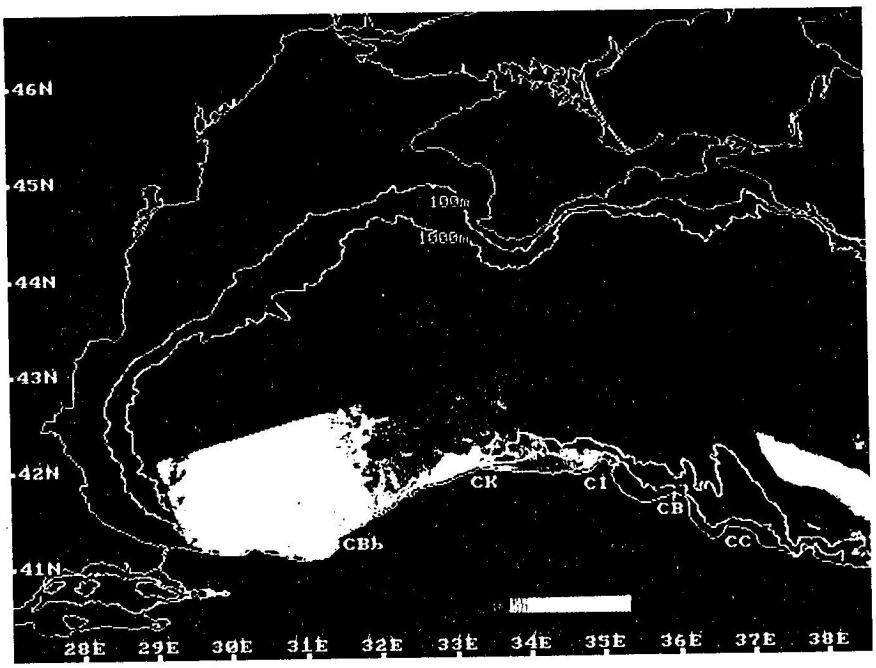

taking the form of filaments. In the remaining images of Figs 15b-e we observe rapidly growing and dissipating filaments, extending ~150km offshore. In Fig. 15c we observe periodic wave motion along the coast from Cape Baba to Cape Kerempe, growing rapidly into filaments during the next two days until Fig. 15d.

The fact that upwelling takes place along a coast ordinarily associated with a downwelling circulation of the cyclonic boundary current is most remarkable. The upwelling can not be attributed to local winds, because they are not particularly strong or favourable in summer (e.g. the summer winds at Sinop, largely sea-breezes, are mainly from the northwest).

Although the wind distribution and circulation do not appear to support continuous upwelling along the Anatolian coast, transient dynamics could ressult in the short-term upwelling. For density driven boundary flows, QIU *et al* (1988) found upwelling related reversals of surface salinity near the coast. Similarly, CHAO (1990) indicated upwelling near the coast, even in the case of retrograde fronts. In numerical experiments simulating the Algerian Current (BECKERS and NIHOUL, 1992), a possibility of upwelling was found within anticyclonic eddies as well as within cyclonic ones. Despite the fact that the Algerian Current normally pools low density Atlantic water against the coast, upwelled water occasionally occurs along the coast and within filaments wrapped around coastally attached anticyclonic eddies (MILLOT, 1991).

We note that the upwelling motions start past Capa Baba, and the coldest waters and filaments with greatest offshore extension occur near Cape Kerempe. Despite the lack of *in situ* data showing the flow structure at the time of these observations, we may speculate that the local dynamics, e.g. headland geometry and widening topography, rather than wind forcing, are largely responsible for creating the Anatolian coastal upwelling. We recognise the effects of the widening topography near Cape Kerempe leading to the flow separation observed two months earlier in Figs 9 and 13.

Sharp corners in coastline geometry can lead to localized upwelling, even in the case of buoyant boundary currents with the coast on the right hand side, as shown by CHERNIAWSKY and LEBLOND (1986). Most observations of topographically or geometrically induced upwelling elsewhere have been obtained either near permanent upwelling fronts (e.g. the California coast, IKEDA and EMERY, 1985; NARIMOUSA and MAXWORTHY, 1985, 1987; the southeastern coast of the USA, JANOWITZ and PIETRAFESA, 1982), or under conditions of favorable winds (e.g. the Gulf of Lions, HUA and THOMASSET, 1983).

Similar upwelling is observed in the available AVHRR images of the summers of 1990, 1991 and 1992 (Figs 16-20). *In situ* data during some of these periods are used to verify the upwelling features.

On June 20, 1990 and the following August 22 1990 images (Figs 16a,b) cold water patches can be seen along the Anatolian coast. The August 29, 1990 image (Fig.16c) shows the development of a wave-like feature (wavelength ~100km) with regularly spaced offshore filaments (10-20km wide and ~70km long) of cold water in the region between Sakarya Canyon and Cape Ince. We also note the similarity of the wave-like features occurring in the same area, in the two images of August 29, 1980 (Fig.15c) and August 29, 1990 (Fig.16c) taken at the same time of the year. We have *in situ* data observed later, in September 1990, which indicate anticyclonic recirculation in the region of Cape Kerempe to Cape Bafra (OGUZ *et al*, 1993), but there was no indication of cold surface water in the area, perhaps because the upwelling had ceased to exist in the autumn.

Imagery from summer 1991 (Figs 17a,b) similarly indicate upwelling to the east of Cape Kerempe (Figs 20a,b). In just one day, between September 14 and 15, 1991, a large change occurs in the area covered by the upwelled water. Wave-like features with scales of about 100km are evident in Fig.17b. Within the next ten days until the next image on September 24, 1991 (Fig.17c), the upwelling disappeared along the Anatolian coast. This is in agreement with the hydrographic data taken during the later part of September 1991 (Figs 18a,b). Figure 18a shows warm water along the coast in the recirculating area west of Cape Ince, except between Cape Baba and Cape Kerempe where the boundary current is discontinuous as shown by the streamlines in Fig.18b. This region of discontinuous currents could either indicate a coastal attachment of the current not sufficiently resolved by the geostrophic analyses, or they could indicate residual downwelling/ upwelling along the coastline, although the transient events were observed somewhat earlier.

A remarkable feature in Figs 17a-c is the pair of warm water filaments extending from the northeastern (Caucasian) shores towards the interior of the eastern basin, each with a length of ~250km, a width of several tens of km, and horizontal spacing of ~150km. These features are associated with the dynamics of the boundary current in the eastern basin, downstream of the large anticyclone trapped in the southeast corner (a permanent feature found almost every time, including the 1991 and 1992 surveys, Figs 18b and 20b). These features indicate that the interaction between the boundary current and the basin interior is not confined to the western basin, but similar interactions, though with different types of instability, also occur in the eastern basin.

Returning back to the Anatolian upwelling, a persistent summer event of long duration is evident in infra-red images of August-September 1992 (Figs 19a-c). Data obtained by the R/V *Bilim* (Figs 20a-c) indicate that the upwelling occurred earlier during July 1992. Both the survey data and the APT image obtained in early August indicated the upwelling region to be small. The *in situ* data located its centre west of Cape Ince, and infrared image located it near Cape Kerempe. In the AVHRR images later in August, the upwelling region had grown in size, covering the entire region from Cape Baba to Cape Ince. Periodicity in the upwelling features is evident in the last image.

The surface temperature distribution (Fig.20a) indicates a cold water patch between Cape Kerempe and Cape Ince with a temperature of 10°C at its center (compared to surface temperatures

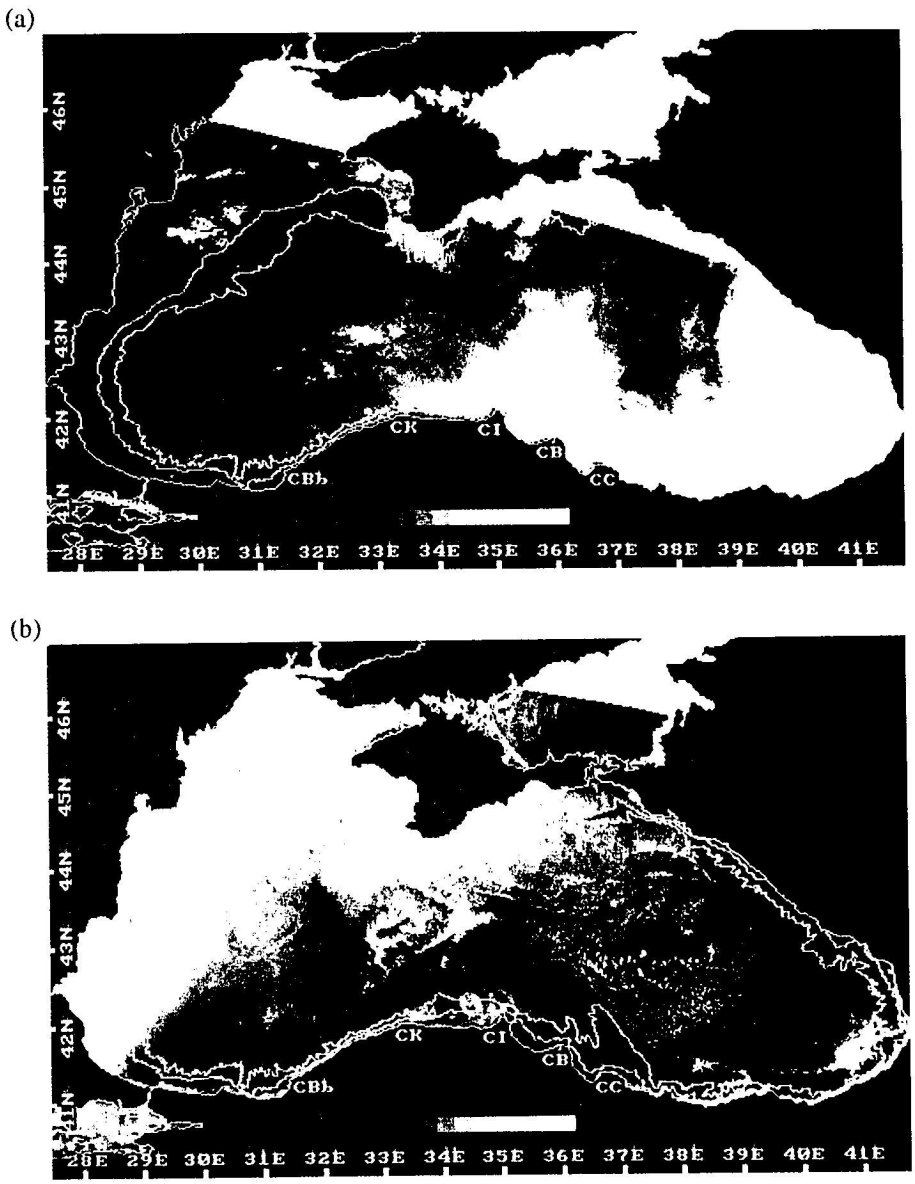

FIG.16. Advanced Very High Resolution Radiometer (AVHRR) satellite images on (a) June 20, (b) August 22, and (c) August 30, 1990 representing the atmospherically uncorrected (NOAA-10) channel 4.

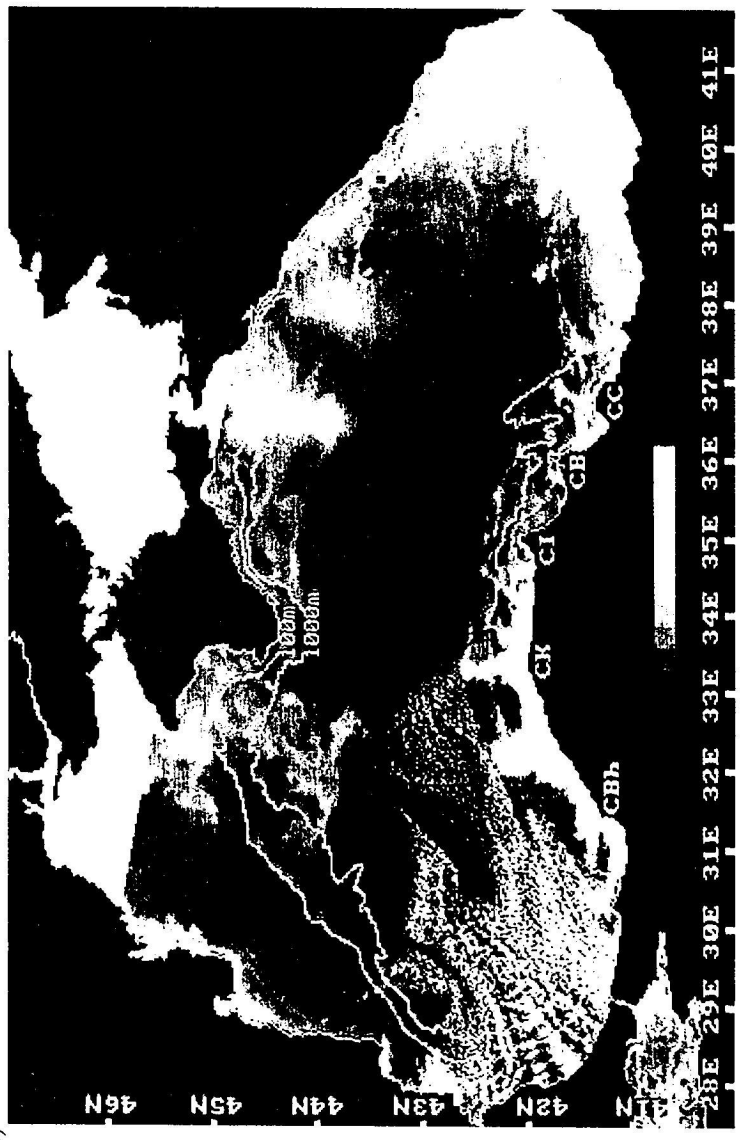
28E
29E
30E
31E
32E
33E
34E
35E
36E
37E
38E
39E
40E
41E
41N
42N
43N
44N
45N
46N
100m
200m
CK
CI
CB
CC
CBb

(c)

(a)

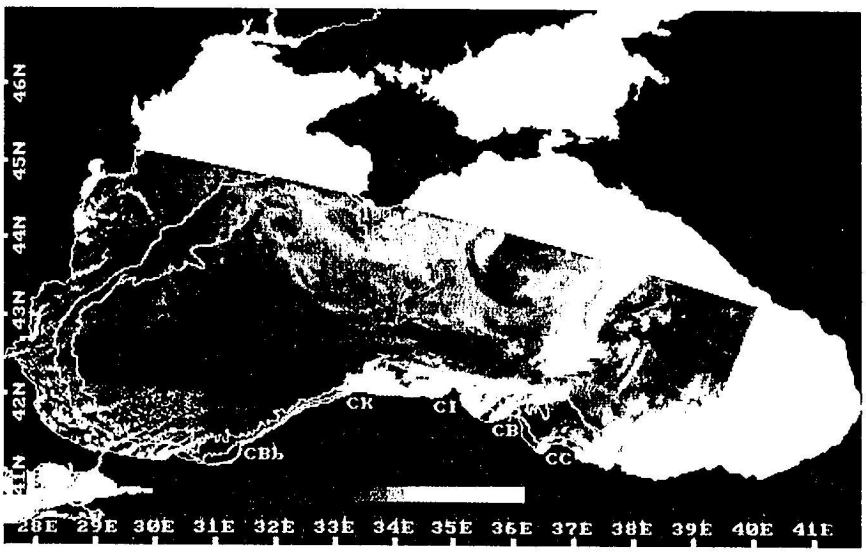

(b)

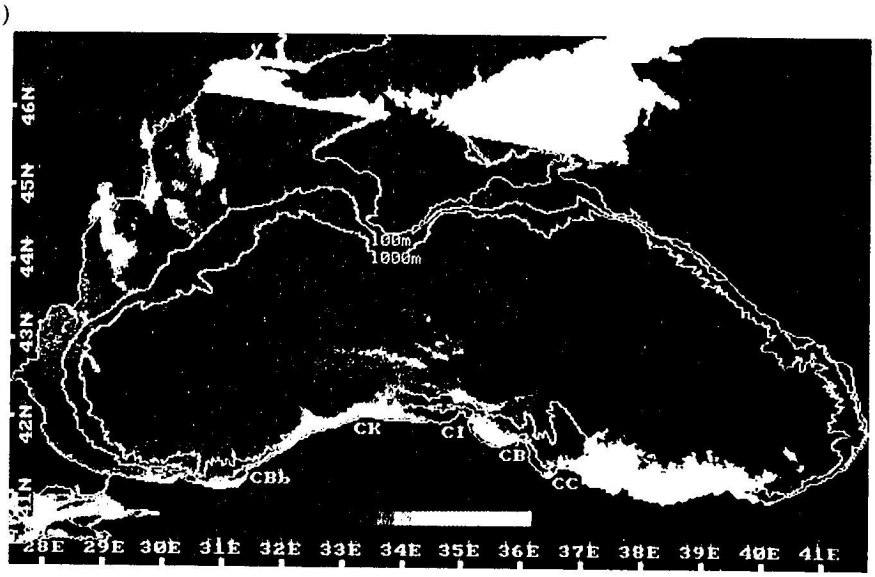

FIG. 17. Advanced Very High Resolution Radiometer (AVHRR) satellite images on (a) September 14, (b) September 15 and (c) September 24, 1991, representing the atmospherically uncorrected (NOAA-10) channel 4.

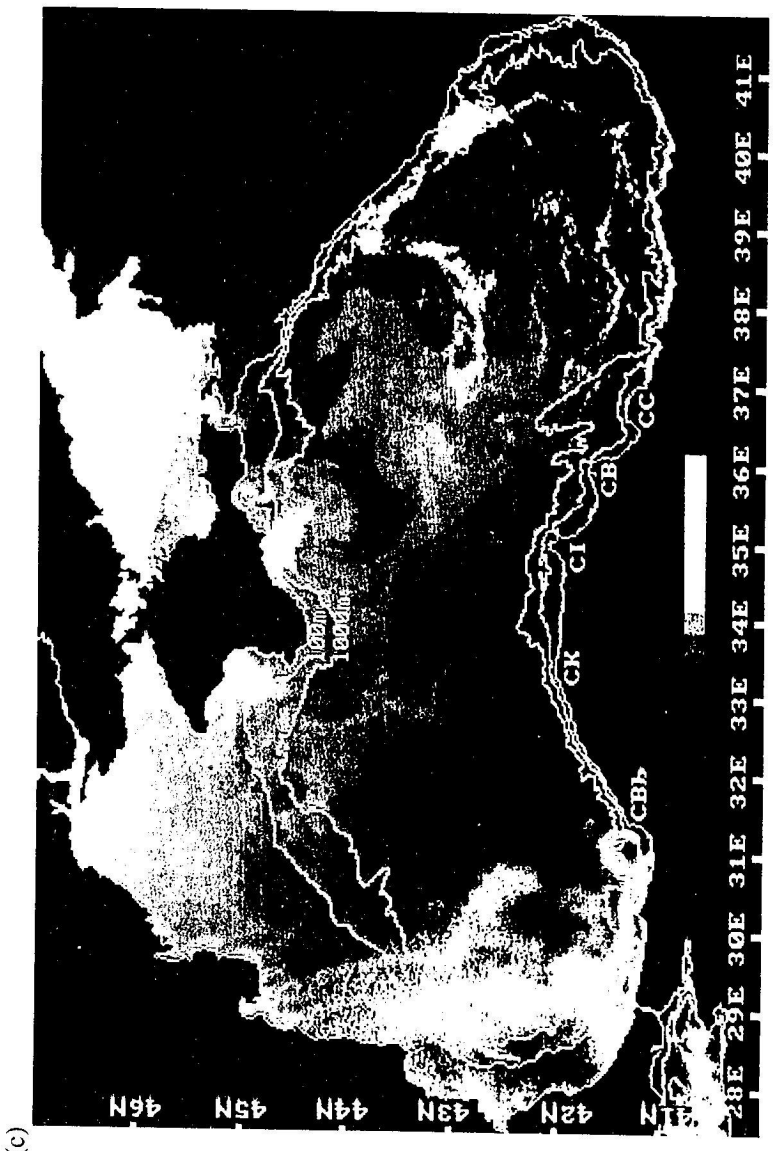
46N
45N
44N
43N
42N
41N
28E
29E
30E
31E
32E
33E
34E
35E
36E
37E
38E
39E
40E
41E
CK
CI
CB
CC
CB1
100m
1000m

(c)

(a)

SEPTEMBER 1991

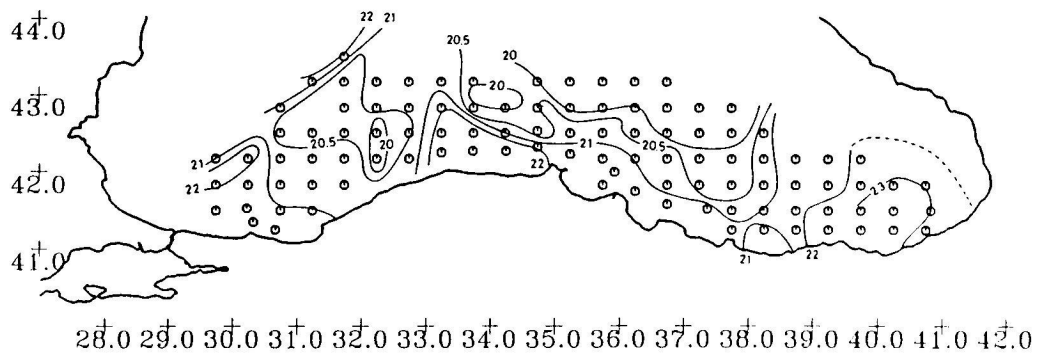

(b)

SEPTEMBER 1991

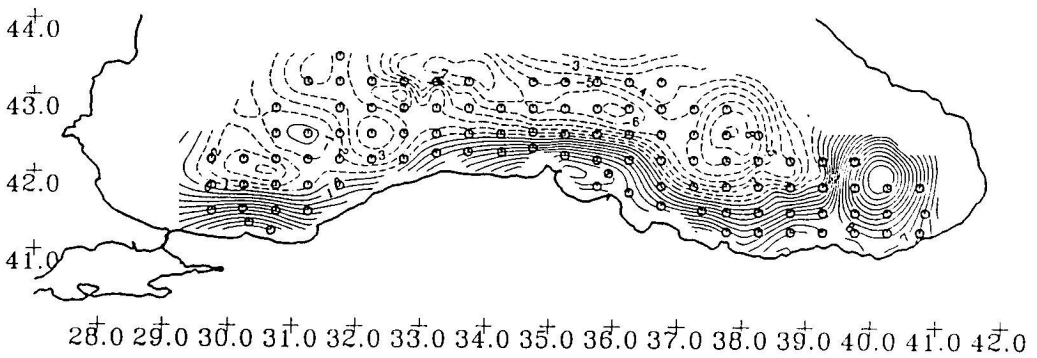

FIG. 18. (a) Surface temperature and (b) surface dynamic topography (cm), referenced to 300m during the September 1991 cruise of the R/V *Bilim*.

of 21-24°C elsewhere). The dynamic topography in Fig.20b displays boundary currents with alongshore variations similar to those indicated in Fig.18b. The current either becomes discontinuous or attached to the coast between Cape Baba and Cape Kerempe, but becomes separated downstream of Cape Kerempe. The cold water patch in Fig.20a occurs at the same location where the streamlines indicate a surface divergence in Fig.20b.

In Fig.20c, the cross-shore transects across the cold water patch show a localized structure with upwelling at its centre. Note that there are three layers of density: at the base of the shallow mixed layer density gradients are dominated by the contribution of the vertical gradient of temperature; below this, the permanent core of the Cold Intermediate Water (ÖZSOY *et al*, 1993; OGUZ *et al*, 1992) has minimum temperatures of <7°C at a depth of about 50m. The permanent pycnocline below this layer of cold water is dominated by the contribution of salinity gradients and, in general, slopes down towards the periphery of the basin in accord with the cyclonic basin circulation. Note, however, that the main pycnocline dips down towards the coast at the offshore part of the section in Fig.20c; then a reversal in its slope occurs near the coast, as a result of the upwelling activity. Near the surface, the vertical motions appear at some distance from the coast, leading to the penetration of the thin mixed layer zone by the underlying Cold Intermediate Water. This is perhaps the most favourable condition for upwelling: the shallow (10-20m) mixed layer can expose the underlying cold water when a surface divergence is created by the dynamics of the unstable boundary currents.

Notice that the width of the boundary current increases as it separates from the coast near Cape Kerempe (Fig.20b). This is reminiscent of a shock, or a critical transition, which may be associated with the effects of the Cape. CHERNIAWSKY and LEBLOND (1986) suggested that travelling shocks or bores could be formed near a cape although they predicted that stationary shocks were not possible. NOF (1984) showed that propagating shock waves can be generated along buoyant boundary currents by a sudden increase in the upstream transport.

During the observations of 1990-1991, the upwelling region is variable in character, with rapid changes in total area of the cold water patterns under the influence of local dynamics. Based on a sequence of images for an upwelling filament between Cape Kerempe and Cape Ince, OGUZ *et al* (1992) concluded that the upwelling features do not translate along the coast. Although our observations show rapid changes, the rapidity of creation and dissipation of filaments could mask organized motions. In any case, it is difficult to recognize any phase propagation during upwelling (e.g. Figs 14c and 15a-3). This apparently static nature of the patterns would be consistent with recirculation shoreward of the separated boundary current east of Cape Kerempe (Fig.13), and with the relatively smaller current velocities to the west of it (Figs 18b and 20b). We also speculate that the upwelling is usually observed in summer, when the relaxation in the strength of the circulation (e.g. STANEV, 1990) could create conditions favourable for upwelling.

Measurements during the detailed survey of July 1992 (NIERMANN, BINGEL, GORBAN, GORDINA, GÜCÜ, KIDEYS, KONSULOV, RADU, SUBBOTIN and ZAIKA (1993) indicate that only very few eggs and larvae of Anchovy were found in the cold water patch of Fig.20a, although they were abundant elsewhere. At the same location both phyto- and zoo-plankton were present in the near surface layers; in fact some yet unidentified species of phytoplankton and some copepods (especially the cold water species *Pseudocalanus elongatus*) were more abundant in the cold water patch, as compared to the surroundings. The decreased abundance of ichtyoplankton, despite a presence of phyto- and zoo-plankton, in the cold water patch seems to suggest that either the spawning of anchovy was suppressed, or the eggs and larvae could not survive the temperature shock created by the cold, upwelled waters.

It is worth noting that the same situation also occurred during a survey in July 1957 (EINARSSON

(a)

FIG. 19. (a) Automatic Picture Transmission (APT) infra-red image on August 4, 1992 (NOAA-10) without atmospheric and geometric corrections, (b) and (c) AVHRR (NOAA-11) infra-red images on August 30 and September 3, 1992, respectively. Lighter shades correspond to colder temperatures in satellite imageries. The AVHRR imageries were supplied by Paul Gerdeers from the Royal Netherlands Meteorological Institute (KNMI).

(b)

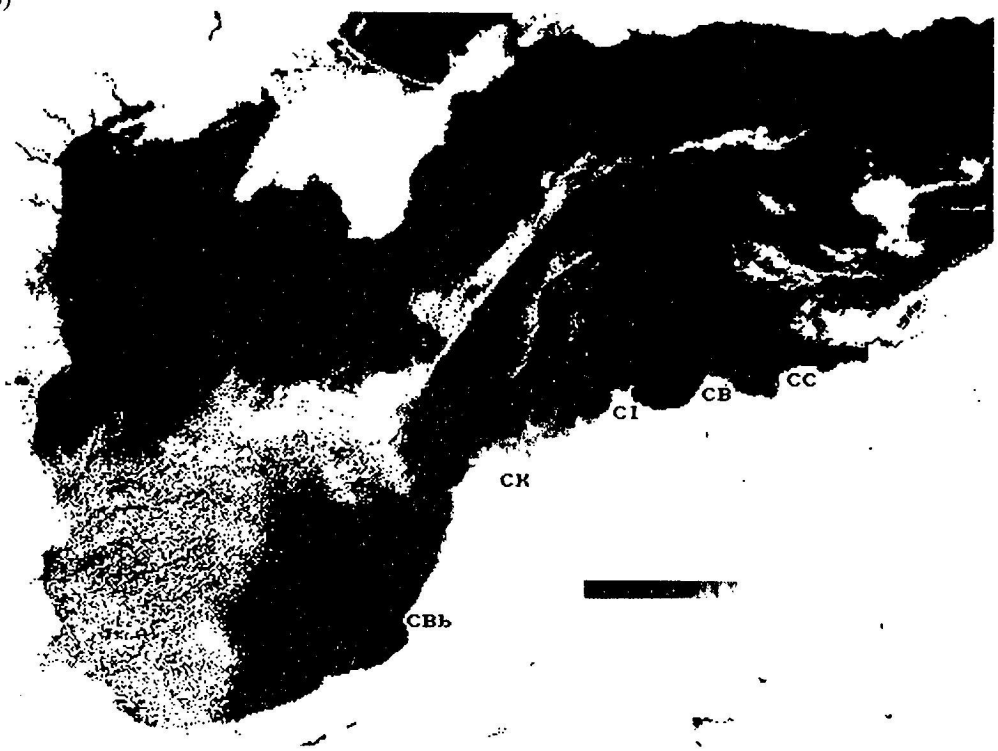

(c)

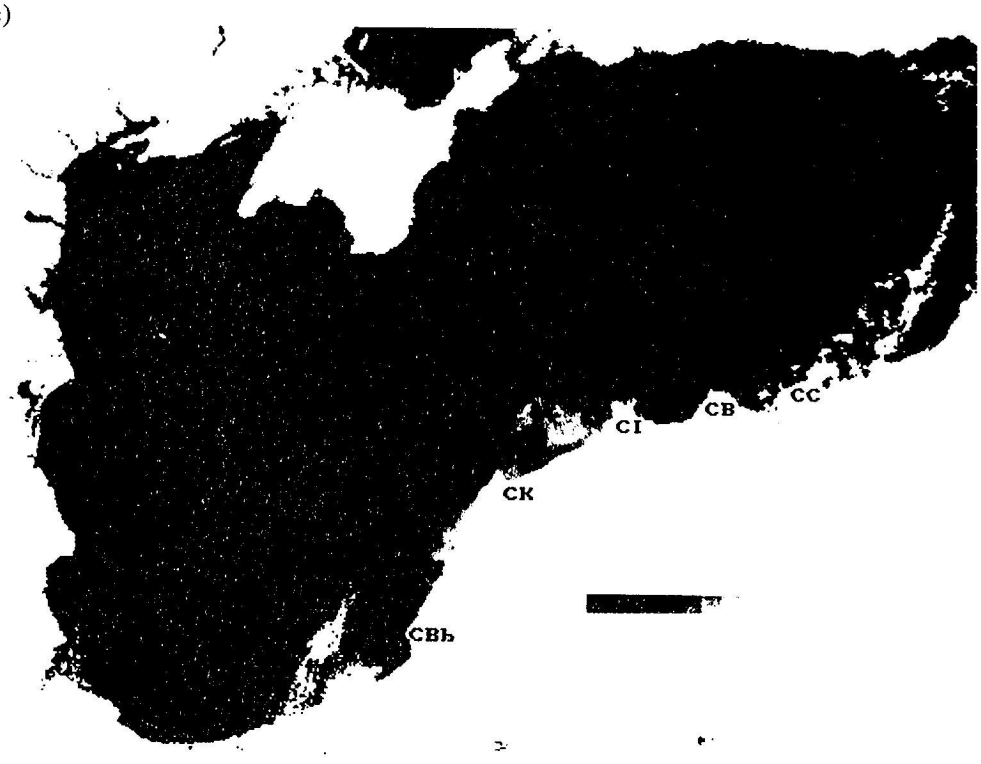

(a)

JULY 1992

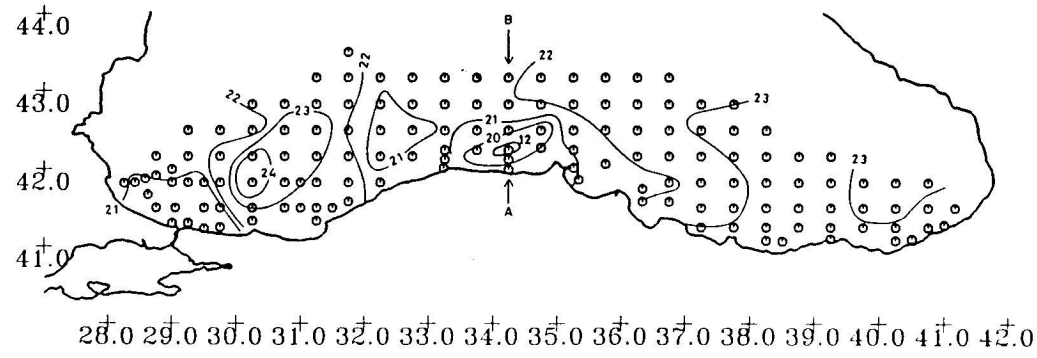

(b)

JULY 1992

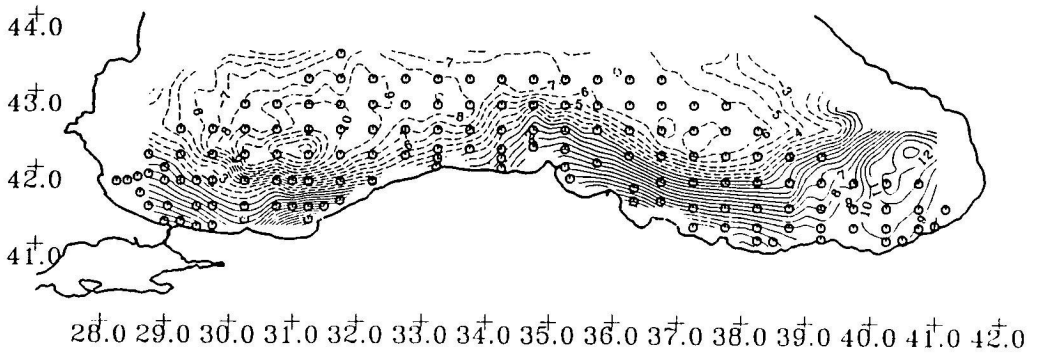

FIG.20 (a) Surface temperature (°C), (b) dynamic topography (cm) referenced to 300m, and (c) the distribution of properties on a cross-shore transect passing through the upwelling region marked in (a), during the July 1992 cruise of the R/V *Bilim*.

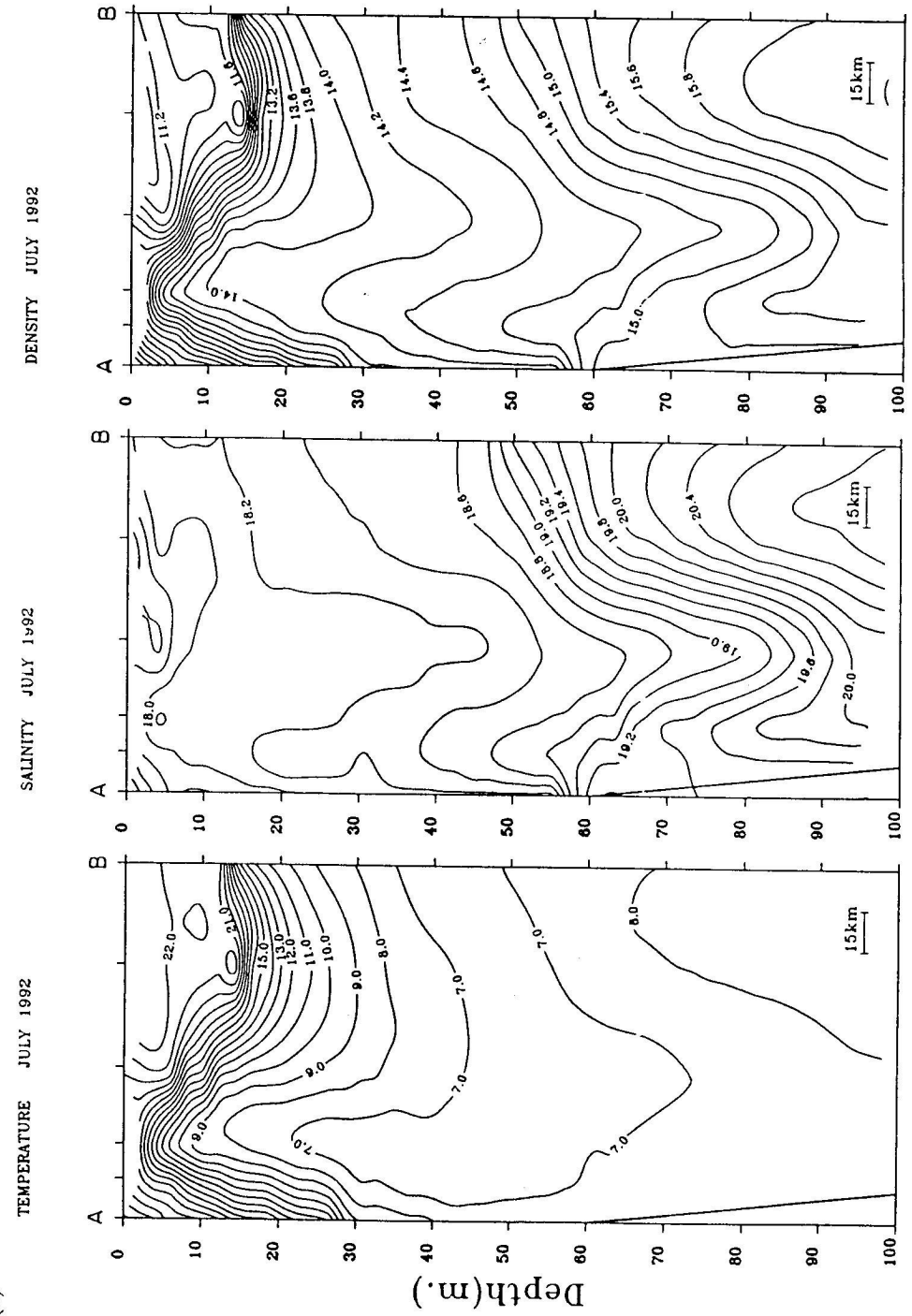
TEMPERATURE JULY 1992
SALINITY JULY 1992
DENSITY JULY 1992
Depth(m.)
A
B
15km

(c)

and GÜRTÜRK; 1960, NIERMANN *et al*, 1993). In this case, the upwelling region extended from Cape Baba to Cape İnce region, with temperatures as low as 11.6°C (at 10m depth) occurring in the same location as the 1992 upwelling. The distribution of anchovy eggs showed a total lack of eggs in the upwelling region (NIERMANN, *et al*, 1993).

4.4 Winter convection and productivity on the western shelf

Our limited winter data yield unique observations of shelf and slope processes. An infra-red (AVHRR) image on February 27, 1990 (Fig.21) indicates cold water with uniform temperatures along the entire western continental shelf. This well-mixed water has a uniform temperature of ~6.5°C and salinity <18 in the upper 30-40m along the southern coast (Figs 22a,b), and water with similar properties is expected to occupy the shallower part of the northwestern and western shelf regions as witnessed in Fig.21. The width of this band of cold water decreases towards the south, parallel to the decreasing width of the shelf. In fact, it can be verified that the boundary of the cold water follows a constant depth contour between 50 and 100m along the entire western shelf.

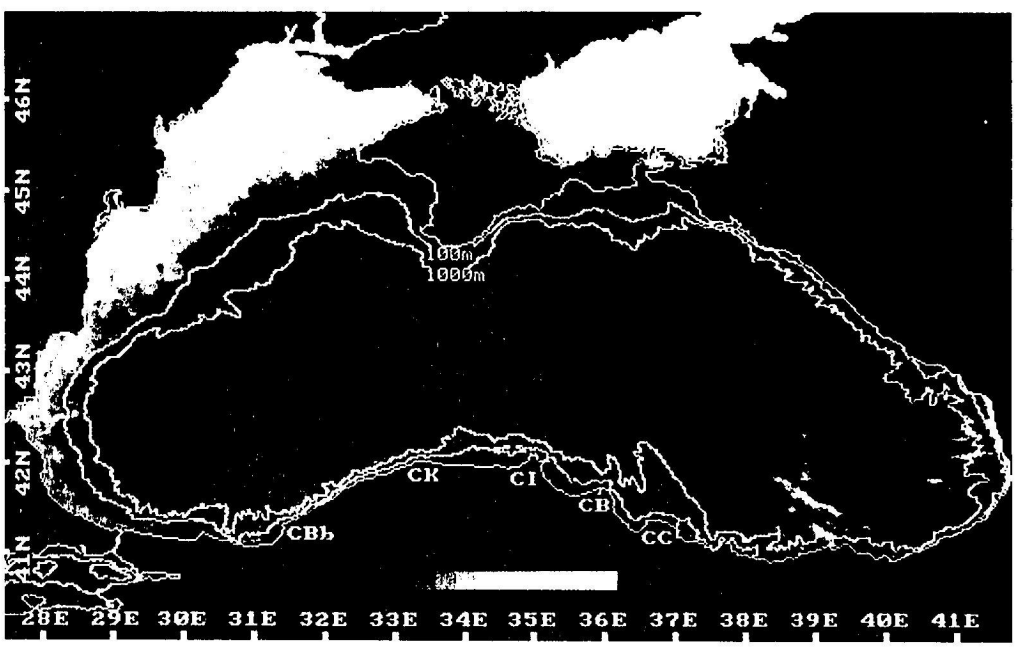

FIG.21. Advanced Very High Resolution Radiometer (AVHRR) satellite image on February 27 1990. The satellite images represent atmospherically uncorrected (NOAA-10) channel 4.

(a)

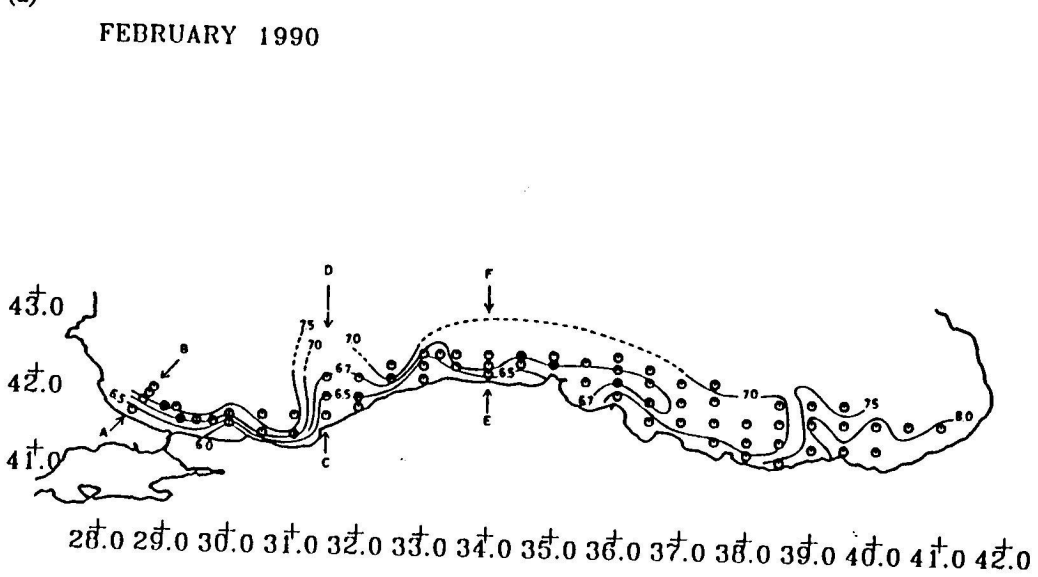

(b)

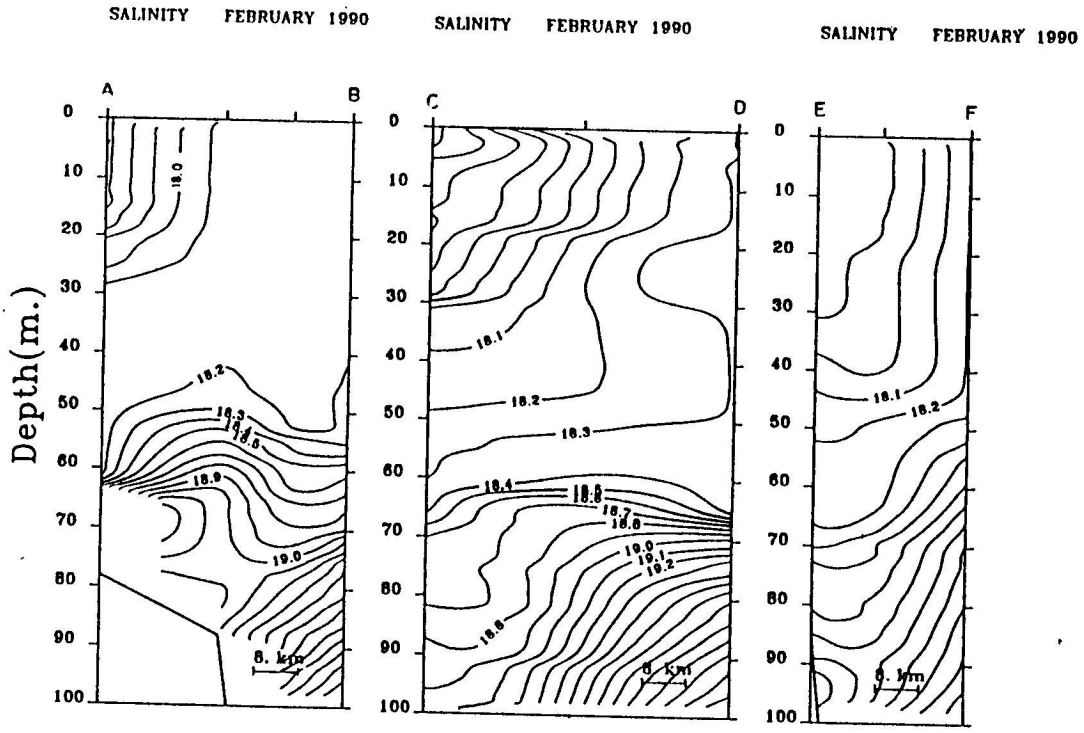

FIG.22. (a) Surface temperature distribution and (b) cross-shore hydrographic sections marked in (a), during the February 1990 cruise of the R/V *Bilim*.

The band of cold water flowing along the western shelf in Fig.21 becomes so thin that it is hardly detectable along the southeastern shelf. Because it is so thin, the cold water hugs the coast and is transported along the shallow inner part (<100m) of the Sakarya Canyon without setting up any disturbance there (compare with Fig.10). When the boundary current transporting the cold water reaches the concave coastline to the east of the Canyon it flows north, and becomes separated from the coast near Cape Baba, where the shallow region suddenly ends. The temperature structure displayed in Figs 21 and 22a near the Cape is most striking: the shape of the front delineating the flow is very similar to a shock; the narrow band of cold water suddenly expands and continues to flow along the coast with a sudden increase in width.

Our review in Section 4.3 of the effects of Sakarya Canyon indicates that the abrupt changes in depth can excite oscillatory motions supplied by baroclinic energy conversions. On the other hand, the possibility of flow separation has been predicted by SPITZ and NOF (1991), for a barotropic flow meeting a sudden depth increase (such as the well-mixed shelf-bound flow of cold water proceeding offshore near Cape Baba in Fig.21). This result is obtained for a coastal jet, keeping all nonlinear terms in the equations of motion. The hydraulics of nonlinear rotating flows seem to have directional preference. ARMI (1989) found an analogy of zonal flows with the hydraulic control theory, with two possible states for the width of an eastward flowing barotropic β-plane jet for a given flux; no controls were found for westward flowing jets (results confirmed by other analyses, e.g. HUGHES, 1985). If the planetary β-effect is exchanged with the effects of topographic slope, we would not expect such hydraulic transitions for a steady jet flowing in the Kelvin wave propagation direction, i.e. with the coast on the right. A transition from subcritical to supercritical flow was found in the case of the two-layer coastal jet studied by GILL and SCHUMANN (1979), with combined effects of shelf topography and coastal curvature. However, when their results are translated to the northern hemisphere, they can only be applied for coastal jets bounded by a left hand side coast, in line with the above results for barotropic flows. CHERNIAWSKY and LEBLOND (1986) suggested that for a buoyant boundary current along a coastline, flow separation could occur near sharp re-entrant corners.

For the above reasons, we suspect the sudden expansion at Cape Baba is the result of the flow separation as it crosses into the deep water region and turns around the corner made by the coastline, rather than a steady state hydraulic transition.

It is also important to recognise the relation of the cold shelf water relative to the boundary current system in Fig.21. Note that a band of warm water is present along the northern and eastern boundaries in this winter image of the Black Sea. Along the western and southern coasts, the warm water occurs along the continental slope offshore of the shelf waters and gradually disappears through frontal mixing with the cold shelf water. This gradual blending of cold and warm waters proceeds along the coast from west of Crimea to near Cape Baba on the Anatolian coast where the expanded ribon of cold water mixes efficiently with the warm slope waters. As a result, the tongue of cold water diminishing towards the east and its separation from the coast after Cape Ince is evident in Fig.22a.

Phytoplankton counting along the Turkish coast during February 1990 indicated an intense bloom along the coast, first following the ribbon of cold water to Cape Baba, and then in the separated flow region up to Cape Kerempe, in the same area as the cold water is seen in the satellite image. Throughout the survey area, the diatom *Chaetoceros sp.* was dominant, having abundances amounting to >91% of the total phytoplankton population of size >55μm. This percentage increased further in the coastal area adjacent to Cape Baba. The total number of individuals increased logarithmically to ($>10^6$ cells l^{-1}) near the coast at Cape Baba, but then decreased gradually towards the east. In the same region, there was a parallel increase of the observed number

of species near the coast (54 coastal species versus ~10 offshore species; species richness index increasing from a value of 1.2 in the offshore region to about 3.8 near the coast), but the corresponding measures of diversity decreased abruptly within the coastal band of cold water (Shannon-Weaver index <0.1, evenness index ~0.02) as compared to the offshore regions (Shannon-Weaver index >1.0, evenness index >0.5) (UYSAL, 1993). It is not clear whether this high abundance of dominant phytoplankton species was linked with the transport of plankton from the northwest shelf, local production resulting from nutrients either supplied via the ribbon of cold water, or entrained from the deep water. It is also not clear whether such a winter bloom supports higher trophic levels or collapses rapidly by sedimentation.

5. SUMMARY AND CONCLUSIONS

Relative to remotely-sensed thermal images which yield data restricted to a thin layer of surface water influenced by short-term surface heat fluxes, the CZCS data for the Black Sea have greatly enhanced value in producing depth-integrated signature of the available colour tracers, faithfully reproducing the transport patterns of the underlying flow dynamics. We have used phytoplankton pigment and particulate fields of CZCS together with or separately from infra-red images to study the current structures, the distribution of competing species of phytoplankton productivity and the progression of eutrophication in the Black Sea.

It is evident that materials originating from lateral sources are transported by the boundary current flowing along the continental slope topography, and are later dispersed along the coast and across frontal region by turbulent, meandering motions. These unstable motions, translating eastward along the Anatolian coast, are initiated by interactions with the sharp topographic variations in the along-shore direction. Flow separation caused by widening shelf topography or headlands is also evident, and influences the transport and vertical motions along the coast.

Upwelling is revealed, with rapidly varying distribution along a particular stretch of the Turkish coast, and persisting for extended periods in summer. However, the basic mechanism leading to upwelling remains largely unexplained. We suggest that interactions of the current system with the coastline geometry and bathymetry induces upwelling without any need for wind forcing to be present.

The advection of materials along the periphery of the basin and the cross-shelf transports created along the boundary current are important for the spreading of productivity and the subsequent basin-scale eutrophication processes, and sets the time and space scales of a succession of plankton blooms and their transformation into higher trophic levels. It is also recognised that these circulation features are important for the migration/spawning behaviour of the mainly pelagic fish stocks of the Black Sea, although they are now under an increasing threat of extinction. Only a better understanding of the system and a massive effort by collaborating European and Asian states to control their harmful effluxes can save *Pontos Euxeinos* (i.e. the hospitable sea, named after the early Greek civilisations and trading colonies who inhabited its coasts).

6. ACKNOWLEDGEMENTS

This study was made possible through the TU-Fisheries Project of the NATO Science for Stability Program, and partially funded by the Turkish Scientific and Technical Research Council (TÜBITAK). We would like to thank Paul Geerders who obtained the AVHRR images for August 1992 from the Royal Netherlands Meteorological Institute (KNMI) and to Paul E. LaViolette, who supplied most of the other level-1 CZCS and AVHRR data as part of a collaborative agreement within the TU-Fisheries project.

7. REFERENCES

Acara, A. (1958) Fluctuation of the surface water temperature and salinity of the Bosphorus. *Rapports et Procès-verbaux des Reunions de la CIESMM*, 15(3), 255-258.

Ahlnäs, K., T.C. Royer and T.H. George (1987). Multiple dipole eddies in the Alaska Coastal Current detected with Landsat Thematic Mapper Data. *Journal of Geophysical Research*, 92, 13041-13047.

Armi, L. (1989) Hydraulic control of zonal currents on a β-plane. *Journal of Fluid Mechanics*, 201, 357-377.

Arnone, R.A. and P.E. La Violette (1986) Satellite definition of the bio-optical and thermal variation of coastal eddies associated with the African Current. *Journal of Geophysical Research*, 91, 2351-2364.

Artüz, M.I. and H.C. Uguz (1976) Daily observations on the hydrographic conditions of the Bosphorus during the period of 1967-1970. *Publications of the Hydrobiology Research Institute, Faculty of Science, University of Istanbul*, 16, 35pp. (in Turkish).

Barale, V. and L. Fusco (1992) Ocean colour, planktonic pigments and productivity. *Rapports et Procès-verbaux des Reunions de la CIESMM*, 33 10.

Bastürk, Ö, A.C. Saydam, I. Salihoglu and A. Yilmaz (1986) Health of the Turkish Straits II: Chemical and environmental aspects of the Sea of Marmara. In: *Oceanography of the Turkish Straits, First Annual Report, Vol.II*, Institute of Marine Sciences, Middle East Technical University, Erdemli, Içel, Turkey. 86pp.

Batchelor, G.K. (1970) *An introduction to Fluid Dynamics*, Cambridge University Press, 615pp.

Beckers, J.M. and J.C.J. Nihoul (1992) Model of the Algerian Current's instability. *Journal of Marine Systems*, 3, 441-451.

Benli, H. (1987) Investigations of plankton distribution in the Southern Black Sea and its effects on particle flux. In: *Particle flux in the Ocean*, E.T. Degens, E. Izdar and S. Honjo, editors, Mitteilungen des Geologisch-Paleontologischen Institut, Universität Hamburg, 62, 77-87.

Blatov, A.S., A.N. Kosarev and V.S. Tuzhilkin (1980) Variability of the hydrographic structure of the Black Sea Water and its links with the external factors. *Vodnyye Resursy* (Water Resources), 6, 71-82, (in Russian).

Blatov, A.S., N.P. Bulgakov, V.A. Ivanov, A.N. Kosarev and V.S. Tuzhilkin (1984). *Variability of hydrophysical fields in the Black Sea.* Hydrometeoizdat, Leningrad, 240pp. (in Russian).

Bologa, A.S. (1986) Planktonic primary productivity of the Black Sea: A Review. *Thalassia Jugoslavica*, 22, 1-22.

Bondar, C. (1989) Trends in the evolution of the mean Black Sea level. *Meteorology and Hydrology* (Romania), 19, 23-28.

Boyer, D.L. and R. Chen (1987) On the formation and shedding of vortices from side-wall mounted obstacles in rotating systems. *Dynamics of Atmospheres and Oceans*, 11, 59-86.

Carstens, T., T.A. McClimans and J.H. Nilsen (1984) Satellite imagery of boundary currents. In: *Remote sensing of shelf sea hydrodynamics*, J.C.J. Nihoul, editor, Elsevier, 235-256.

Coble, G.P., R.B. Gagosian, L.A. Codispoti, G.E. Friederich and J.P. Christensen (1991) Vertical distribution of dissolved and particulate fluorescence in the Black Sea. *Deep-Sea Research*, 38, S985-S1001.

Condie, S.A. (1989) Mesoscale structures on density driven boundary currents. In: *Mesoscale/synoptic coherent structures in geophysical turbulence*, J.C.J. Nihoul and B.M. Jamart, editors, Elsevier, Amsterdam, 197-210.

Chao, S-Y. (1988) Instabilities of fronts over a continental margin. *Journal of Geophysical Research*, 95, 3199-3211.

Cherniawsky, J. and P.H. Leblond (1986) Rotating flows along indented coastlines. *Journal of Fluid Mechanics*, 169, 379-407.

Chirea, R. and T. Gomoiu (1986) Some preliminary data on the nutrient influx into western Black Sea. *Cercetari Marine*, IRCM Constanta, 19, 171-189.

Crepon, M., L. Wald and J.M. Monget (1982) Low-frequency waves in the Ligurian Sea during December 1977. *Journal of Geophysical Research*, 87, 595-600.

Cresswell, G.R. and T.G. Golding (1980) Observations of south-flowing current in the southeastern Indian Ocean. *Deep-Sea Research*, 27, 449-466.

Cushman-Roisin, B. and J.J. O'Brien (1987) The influence of bottom topography on baroclinic transports. *Journal of Physical Oceanography*, 13, 1600-1611.

DESCHAMPS, P.Y. and R. FROUIN (1984) Large diurnal heating of the sea surface observed by the HCMR Experiment. *Journal of Phyusical Oceanography*, 14, 177-184.

DEUSER, W.G. (1971) Organic carbon budget of the Black Sea. *Deep-Sea Research*, 18, 995-1004.

EINARSSON, H. and N. GÜRTÜRK (1960) Abundance and distribution of eggs and larvae of the Anchovy (*Engraulis encrasicholus ponticus*) in the Black Sea (Results of the Pektas Expedition). *Hydrobiological Research Institute, Faculty of Science, University of Istanbul, Series B*, 5(1-2), 79-94 + 2 plates.

EREMEEV, V.N., V.L. VLADIMIROV and B.N. KRASHENINNIKOV (1992) Long-term variability of the Black Sea Water transparency. In: *Hydrophysical and hydrochemical studies of the Black Sea*, Marine Hydrophysical Institute, Ukraine Academy of Sciences, Sevastopol, 28-30.

FEDOROV, K.N. and A.I. GINSBURG (1989) Mushroom-like currents (vortex dipoles); one of the most widespread forms of non-stationary coherent motions in the ocean. In: *Mesoscale/synoptic coherent structures in geophysical turbulence*. J.C.J. NIHOUL and B.M. JAMART, editors, Elsevier, Amsterdam, 1-14.

FEDOROV, K.N., A.I. GINSBURG and A.G. KOSTIANOV (1989) Modelling of 'mushroom-like' currents (vortex dipoles) in a laboratory tank with rotating homogeneous and stratified fluids. In: *Mesoscale/synoptic coherent structures in geophysical turbulence*, J.C.J. NIHOUL and B.M. JAMART, editors, Elsevier, Amsterdam, 15-24.

FONSELIUS, S.H. (1974) Phosphorus in the Black Sea. In: *The Black Sea - Geology, Chemistry, Biology*. American Association of Petroleum Geologist, Memoir No.20, 144-150.

GAMSAKHURDIYA, G.R. and A.S. SARKISYAN (1976) Diagnostic calculations of current velocities in the Black Sea. *Oceanology*, 15, 164-167.

GILL, A.E. and E.H. SCHUMANN (1979) Topographically induced changes in the structure of an inertial coastal jet: Application to the Agulhas Current. *Journal of Physical Oceanography*, 9, 975-991.

GINSBURG, A.I. and K.N. FEDOROV (1989) On the multitude of forms of coherent motions in Marginal Ice Zones (MIZ). In: *Mesoscale/synoptic coherent structures in geophysical turbulence*. J.C.J. NIHOUL and B.M. JAMART, editors, Elsevier, Amsterdam, 25-40.

GÖÇMEN, D. (1988) *Fluctuations of chlorophyll a and primary productivity as related to physical chemical and biological parameters in Turkish coastal waters*. MS Thesis, METU, Institute of Marine Sciences, Erdemli, Içel, Turkey, 137pp.

GORDON, H.R., O.B. BROWN, R.H. EVANS, J.W. BROWN, R.C. SMITH, KI.S. BAKER and D.K. CLARK (1988) A semianalytic model of ocean colour. *Journal of Geophysical Research*, 93, 10909-10924.

GRIFFITHS, R.W. and P.F. LINDEN (1981) The stability of buoyancy-driven coastal currents. *Dynamics of Atmospheres and Oceans*, 5, 281-306.

GRIFFITHS, R.W. and A.F. PEARCE (1985) Instability and eddy pairs on the Leeuwin Current south of Australia. *Deep-Sea Research*, 32, 1511-1534.

HAIDVOGEL, D., A. BECKMANN and K. HEDSTRÖM (1991) Dynamical simulations of filament formation and evolution in the coastal transition zone. *Journal of Geophysical Research*, 96, 15017-15040.

HÄKKINEN, S. (1987) Feedback between ice flow, barotropic flow and baroclinic flow in the presence of bottom topography. *Journal of Geophysical Research*, 92, 3807-3820.

HAY, B.J. and S. HONJO (1989) Particle deposition in the present and holocene Black Sea. *Oceanography*, 2, 26-31.

HAY, B.J., S. HONJO, S. KEMPE, V.A. ITEKKOT, E.T. DEGENS, T. KONUK and E. IZDAR (1990) Interannual variability in particle flux in the southwestern Black Sea. *Deep-Sea Research*, 37, 911-928.

HAY, B.J., M.A. ARTHUR, W.E. DEAN and E.D. NEFF (1991) Sediment deposition in the late holocene abyssal Black Sea: Terrigenous and biogenic matter. *Deep-Sea Research*, 38, (Suppl), S1211-S1235.

HOFFMANN, E.E., K. HEDSTRÖM, J. MOISAN, D. HAIDVOGEL and D.L. MACKAS (1991) Use of simulated drifter tracks to investigate general transport patterns and residence times in the coastal transition zone. *Journal of Geophysical Research*, 96, 15041-15152.

HOLLIGAN, P.M., M. VIOLLIER, D.S. HARBOUR, P. CAMUS and M. CHAMPAGNE-PHILIPPE (1983) Satellite and ship studies of coccolithophore production along a continental shelf edge. *Nature*, 304, 339-342.

HOLLIGAN, P.M., T. AARUP and S.B. GROOM (1989) The North Sea: Satellite colour atlas. *Continental Shelf Research*, 9, 667-765.

HUA, B-L. and F. THOMASSET (1983) A numerical study of coastline geometry on wind-induced upwelling in the Gulf of Lions. *Journal of Physical Oceanography*, 13, 678-694.

HUGHES, R.L. (1985) On inertial currents over a sloping continental shelf. *Dynamics of Atmospheres and Oceans*, 9, 49-73.

HUTHNANCE, J.M. (1992) Extensive slope currents and the ocean-shelf boundary. *Progress in Oceanography*, **29**, 161-196.

IKEDA, M. (1984) Coastal flows driven by a local density flux. *Journal of Geophysical Research*, **89**, 8008-8016.

IKEDA, M. (1987) Modelling interpretation of the ice edge off the Labrador coast observed in NOAA satellite imagery, Northern California. *Journal of Physical Oceanography*, **17**, 1468-1483.

IKEDA, M. and M.J. EMERY (1985) Observation and modelling of meanders in the California Current System off Oregon and Northern California. *Journal of Physical Oceanography*, **14**, 1434-1450.

IKEDA, M., L.A. MYSAK and W.J. EMERY (1984) Observation and modelling of satellite-sensed meanders and eddies off Vancouver Island. *Journal of Physical Oceanography*, **14**, 3-21.

IKEDA, M., J.A. JOHANNESSEN, K. LYGRE and S. SANDVEN (1989) A process study of mesoscale meanders and eddies in the Norwegian coastal current. *Journal of Physical Oceanography*, **19**, 20-35.

JANOWITZ, G.S. and L.J. PIETRAFESA (1982) The effects of alongshore variation in bottom topography on a boundary current. *Continental Shelf Research*, **1**, 123-141.

JOHANNESSEN, J.A., E. SVENDSEN, O.M. JOHANNESSEN and K. LYGRE (1989) Three-dimensional structure of mesoscale eddies in the Norwegian coastal current. *Journal of Physical Oceanography*, **19**, 3-19.

JOHANNESSEN, O.M., J.A. JOHANNESSEN, E. SVENDSEN, R.A. SCHUCHMAN, W.J. CAMPBELL and E. JOSBERGER (1987) Ice-edge eddies in the Fram Strait marginal ice zone. *Science*, **236**, 427-429.

KNIPOVICH, N.M. (1993) Hydrologic research in the Black Sea. *Trudy Azovo-Chernomorskoi Nauchnopromsylovoy Expeditsii*, **10**, 274pp (in Russian).

KOBLENTZ-MISIKE, O.J., V.V. VOLKOVINSKY and J.G. KABANOVA (1970) Plankton primary production of the world ocean. In: *Scientific exploration of the South Pacific*, W.S. WOOSTER, editor, National Academy of Sciences, Washington, 183-193.

LATUN, V.S. (1990) Anticyclonic eddies in the Black Sea in summer 1984. *Soviet Journal of Physical Oceanography*, **1**, 279-286 (in Russian).

LEAMAN, K.D. and R.L. MOLINARI (1987) Topographic modification of the Florida Current by Little Bahama and Great Bahama Banks. *Journal of Physical Oceanography*, **17**, 1724-1736.

LEGECKIS, R. and G. CRESSWELL (1981) Satellite observations of sea surface temperature fronts off the coast of Western and Southern Australia. *Deep-Sea Research*, **28**, 279-306.

MARCHUK, G.I., A.A. KORDZADZE and Y.N. SKIBA (1975) Calculation of the basic hydrological fields in the Black Sea. *Fizika Atomosfery: Okeana, Izvestiya Academiya nauk USSR*, **11**(4), 379-393 (in Russian).

MCCLAIN, E.P., W.G. PICHEL, C.C. WALTON, Z. AHMAD and J. SUTTON (1982) Multichannel improvements to satellite-derived global sea surface temperatures. *Advances in Space Research*, **2**, 43-47.

MEE, L.D. (1992) The Black Sea in crisis: The need for concerted international action. *Ambio*. **21**, 278-286

MIED, R.P., J.C. MCWILLIAMS and G.J. LINDEMANN (1991) The generation and evolution of mushroom-like vortices. *Journal of Physical Oceanography*, **21**, 489-510.

MILLOT, C. (1985) Some features of the Algerian Current. *Journal of Geophysical Research*, **90**, 7169-7176.

MILLOT, C. (1991) Mesoscale and seasonal variabilities of the circulation in the western Mediterranean. *Dynamics of Atmospheres and Oceans*, **15**, 179-214.

MOSKALENKO, L.V. (1976) Calculation of stationary wind driven currents in the Black Sea. *Oceanology*, **15**, 168-171.

MURRAY, J.W. (1991) (editor) Black Sea oceanography, results from the 1988 Black Sea Expedition. *Deep-Sea Research*, **38**, Supplementary Issue 2A, S665-S1266.

MURRAY, J.W. and E. IZDAR (1989) The 1988 Black Sea Oceanographic Expedition: Overview and new discoveries. *Oceanography*, **2**, 15-21.

MUSAYEVA, E.I. (1985) Mesoplankton near the Bulgarian coast. *Oceanology*, **25**, 647-652.

MYSAK, L.A. and F. SCHOTT (1977) Evidence for baroclinic instability of Norwegian Current. *Journal of Geophysical Research*, **82**, 2087-2095.

NARIMOUSA, S. and T. MAXWORTHY (1985) Two-layer model of shear-driven coastal upwelling in the presence of bottom topography. *Journal of Fluid Mechanics*, **159**, 503-531.

NARIMOUSA, S. and T. MAXWORTHY (1987) A note on the effects of coastal perturbations on coastal currents and fronts. *Journal of Physical Oceanography*, **17**, 1296-1303.

NEUMANN, G. (1942) Das Schwarze Meer. *Zeitschr. Ges. f. Erdkunde*, Berlin, 3, 92-114.

NIERMANN, U., F. BINGEL, A. GORBAN, A.D. GORDINA, A. GÜCÜ, A.E. KIDEYS, A. KONSULOV, G. RADU, A.A. SUBBOTIN and V.E. ZAIKA (1993) Distribution of anchovy eggs and larvae (*Engraulis encrasicolus* Cuv.) in the Black Sea in 1991 and 1992 in comparison to former surveys, ICES, CM1993/H:48, 19pp.

NOF, D. (1984) Shock waves in currents and outflows. *Journal of Physical Oceanography*, 14, 1683-1702.
OKUBO, A. (1980) *Diffusion and ecological problems: Mathematical Models*, Springer-Verlag, 254pp.
OGUZ, T., F. BINGEL and S. TUGRUL (1990) Stock assessment studies for Turkish Black Sea coast. *Technical Report*, METU, Institute of Marine Sciences, Erdemli, Içel, Turkey, 122pp.
OGUZ, T., P.E. LA VIOLETTE and Ü. ÜNLÜATA (1992) The upper layer circulation of the Black Sea: Its variability as inferred from hydrographic and satellite observations. *Journal of Geophysical Research*, 97, 12569-12584.
OGUZ, T., V.S. LATUN, M.A. LATIF, V.V. VLADIMIROV, H.I. SUR, A.A. MARKOV, E. ÖZSOY, B.B. KOTOVSHCHIKOV, V.V. EREMEEV, Ü. ÜNLÜATA (1993) Circulation in the surface and intermediate layers of the Black Sea. *Deep-Sea Research*, 40, 1597-1612.
ÖZSOY, E. (1990) On the seasonally varying control of the Black Sea exchange through the Bosphorus. AGU-ASLO Ocean Sciences Meeting, New Orleans, February 1990. *Eos*, 71.
ÖZSOY, E., Ü. ÜNLÜATA and Z. TOP (1993) The Mediterranean water evolution, material transport by double diffusive intrusions and interior mixing in the Black Sea. *Progress in Oceanography*, 31, 279-320.
ÖZSOY, E., M.A. LATIF, S. TUGRUL and Ü. ÜNLÜATA (1992) Water and nutrient fluxes through the Bosphorus, an exchange between the Mediterranean and Black Sea. In: *Problems of the Black Sea, International Conference*, MHI Sevastopol, Ukraine, Plenary reports, 54-67.
ÖZSOY, E., A. HECHT, Ü. ÜNLÜATA, S. BRENNER, T. OGUZ, J. BISHOP, M.A. LATIF and Z. ROZENTRAUB (1991) A review of the Levantine Basin circulation and its variability during 1985-1988. *Dynamics of Atmospheres and Oceans*, 15, 421-456.
ÖZTURGUT, E. (1966) Water balance of the Black Sea and flow through the Bosphorus. *CENTO Symposium on Hydrology and Water Resources development, Ankara, Turkey, February 1966*. 107-112.
QIU, B., N. IMASATO and T. AWAJI (1988) Baroclinic instability of buoyancy-driven coastal density currents. *Journal of Geophysical Research*, 93, 5037-5050.
ROBINSON, I.S. (1991) *Satellite Oceanography. An introduction for oceanographers and remote-sensing scientists.* Ellis Horwood, 455pp.
SAYDAM, C., S. TUGRUL, Ö. BASTÜRK and T. OGUZ (1992) Identification of the oxic/anoxic interface by isopycnal surfaces in the Black Sea. *Deep-Sea Research*, 40, 1405-1412.
SERPOIANU, G. (1973) Le Bilan Hydrologique de la Mer Noire, *Cercetari Marine, IRCM* No: 5-6, 145-153.
SERPOIANU, G., I. NAE and V. MALCIU (1992) Danube water influence on sea water salinity at the Romanian Littoral. *Rapports et Procès verbaux des Reunions de la CIESMM*. 33, 233.
SHETYE, S.R. and M. RATTRAY (1982) The effect of varying bathymetry on steady zonal equivalent barotropic jets. *Deep-Sea Research*, 29, 17-44.
SIMPSON, J.H. and J. BROWN (1987) The interpretation of visible band imagery of turbid shallow seas in terms of the distribution of suspended particulates. *Continental Shelf Research*, 7, 1307-1313.
SOROKIN, YU. I. (1983) The Black Sea. In: *Estuaries and enclosed seas, ecosystems of the world.* B.H. KETCHUM, editor, Elsevier, 253-292.
SPITZ, Y.H. and D. NOF (1991) Separation of boundary currents due to bottom topography. *Deep-Sea Research*, 38, 1-20.
STANEV, E.V. (1990) On the mechanisms of the Black Sea circulation. *Earth-Science Reviews*, 28, 285-319.
STERN, M.E. (1980) Geostrophic fronts, bores breaking and blocking waves. *Journal of Fluid Mechanics*, 99, 687-703.
SUKHANOVA, I.N., M.V. FLINT, G. HIBAUM, V. KARAMFILOV, A.I. KOPYLOV, E. MATVEEVA, T.N. RAT'KOVA and A.P. SAZHIN (1988) *Exuviaella cordata* red tide in Bulgarian coastal waters (May to June 1986). *Marine Biology*, 99, 1-8.
THOMPSON, R.O.R.Y. (1984) Observations of the Leeuwin Current off Western Australia. *Journal of Physical Oceanography*, 14, 623-628.
THOMSON, R.E. (1984) A cyclonic eddy over the continental margin of Vancouver Island: Evidence for baroclinic instability. *Journal of Physical Oceanography*, 14, 1326-1348.
TOLMAZIN, D. (1985) Changing coastal oceanography of the Black Sea. I: Northwestern shelf. *Progress in Oceanography*, 15, 217-276.
TUGRUL, S., Ö. BASTÜRK, C. SAYDAM and A. YILMAZ (1992) Changes in the hydrochemistry of the Black Sea inferred from water density profiles. *Nature*, 359, 137-139.
TUMANTSEVA, N.I. (1985) Red Tide in Black Sea. *Oceanology*, 25, 99-101.

ÜNLÜATA, Ü. and E. ÖZSOY (1986) Health of the Turkish Straits I: Oxygen deficiency of the Sea of Marmara. *Oceanography of the Turkish Straits, First Annual Report Vol. II*, Institute of Marine Sciences, Middle East Technical University, Erdemli, Içel, Turkey, 82pp.

UYSAL, Z. (1993) *A preliminary study on some plankters along the Turkish Black Sea coast: Species composition and spatial distribution.* PhD Thesis, Institute of Marine Sciences, Middle East Technical Universioty, Erdemli, Içel, Turkey. 138pp.

VOROPAYEV, S.I. (1989) Flat vortex structures in a stratified fluid. In: *Mesoscale/Synoptic coherent structures in geophysical turbulence.* J.C.J. NIHOUL and B.M. JAMART, editors, Elsevier, Amsterdam, 671-690.

VAN HEIJST, G.J.F. and J.B. FLOR (1989) Laboratory experiments on dipole structures in a stratified fluid. In: *Mesoscale/Synoptic coherent structures in geophysical turbulence.* J.C.J. NIHOUL and B.M. JAMART, editors, Elsevier, Amsterdam, 591-608.

YENTSCH, C.S. (1984) Satellite representation of features of ocean circulation indicated by CZCS colorimetry. In: *Mesoscale/Synoptic coherent structures in geophysical turbulence.* J.C.J. NIHOUL and B.M. JAMART, editors, Elsevier, Amsterdam, 336-354.

ZAITSEV, YU.P. (1991) Cultural eutrophication of the Black Sea and other South European Seas. *Lamer (Societé franco-Japanaise d'océanographie, Tokyo)*, 29, 1-7.

8. APPENDIX A

PROCESSING AND INTERPRETATION OF CZCS AND AVHRR SATELLITE IMAGES

The Nimbus-7 CZCS is a six channel, multispectral scanning sensor with visible channels (1-5) at 443±10, 520±10, 550±10, 670±10, 700-800nm and one infra-red channel of 10.5-12.5μm (ROBINSON, 1991). The satellite acquired data at about 11:00 (local solar time) each day near the Black Sea.

The bio-optical properties derived from CZCS are assumed to be integrated over one attenuation depth of visible light (ARNONE and LA VIOLETTE, 1986), typically on the order of 25m for open ocean waters and 5m for coastal waters (probably smaller in the case of the Black Sea).

The CZCS visible bands yield information on chlorophyll *a*, a most abundant constituent of live phytoplankton, with strong absorbance in the blue (443nm) and secondarily in the red (670nm) bands of the light spectrum. Accessory pigments have absorption maxima in the green (520nm) and yellow (550nm) bands. The measured reflectance in these bands also depends on the visible light scattering properties of the particulates, especially in the case of diatoms and coccolithophores (HOLLIGAN *et al* 1983). In coastal waters, suspended particulates backscatter in a wide band (channels 1-3 of CZCS) of the visible spectrum (SIMPSON and BROWN, 1987). In low salinity (<30) waters, reflectance can result from dissolved organic matter (DOM) or yellow substance of terrestrial or marine origin (HOLLIGAN, AARUP and GROOM, 1989).

The atmospheric correction algorithm for CZCS images involves the subtraction of a weighted measure of atmospheric aerosol concentration (channel 4, 670nm), and a signal proportion to the Rayleigh (molecular) scattering. The corrected upwelling radiance from the ocean surface is then computed for the first three channels (GORDON, BROWN, EVANS, BROWN, SMITH, BAKER and CLARK, 1988).

The AVHRR data obtained from the thermal infra-red sensors of NOAA-9 and NOAA-11 satellites are calibrated and atmospherically corrected utilizing the AVHRR channels 4 (10.3-11.3nm) and 5 (11.5-12.5nm), and the split-window multichannel technique developed by MCCLAIN, PICHEL, WALTON, AHMAD and SUTTON (1982).